AVIATION ACCIDENTS AETIOLOGY FROM CATASTROPHE THEORY POINT OF VIEW

Maciej Lasek[*], Krzysztof Sibilski[,!], Józef Żurek[**]**
[*]The State Commission of Aircraft Accidents Investigation, Warsaw, Poland,
[**]Air Force Institute of Technology, Warsaw, Poland
[!]Faculty of Power and Mechanical Engineering, Wroclaw University of Technology, Wroclaw Poland

Keywords: *Theory of Catastrophe, Aircraft Accidents Reconstruction, Aviation Safety, Flight Dynamics Modeling and Simulation*

Abstract

Human error is often cited as a major contributing factor or case of incidents and accidents. Reason proposes a view that many accidents are catalyzed by persons not present at the time of the event. In fact, it is this source of latent conditions that pose a most significant threat to the safety of complex system. Another dimension to human error in aviation are the active errors that can precipitate the alignment or trigger the latent conditions. The risk associated with aviation is a dynamic element that is affected by both latent conditions and significant factors. In our opinion this dynamics nature of risk in aviation can be described in terms of Theory of Catastrophe. Using Reason's latent failure model, we try to describe this dynamics nature using the cusp catastrophe model. In our opinion the descriptive and predictive nature of cusp catastrophe model works as a map to illustrate the nature of aviation accidents in terms of "instability" resulting from the alignment of latent conditions and influence of active errors.

1. Introduction

Problems connected with reconstruction of aircraft crashes were the subjects of many works. One can mention here works by Calkins [15], Ditenberger, Haines and Luers [23], Luers and Ditenberger [54], Maryniak [57, 58, 59]. The works mentioned above contained analyses and simulations of specific occurrences. A very interesting work is treatise [15] containing reconstruction of a crash of Boeing 737-300 airliner no. N513AU belonging to USAir airlines (flight 427). The crash took place near Pittsburgh (the aeroplane fell near the town of Aliquippa, Pennsylvania) on September 8th 1994 [79]. Official statement of the commission of investigating aircraft crashes said that the direct cause of the crash was uncontrolled descents which lead to hitting the ground[1]. Calkins showed that the loss of control over the aircraft could have been caused by a vortex flowing off the wings of a Boeing 747 airliner flying in front of N513AU aeroplane. The effect of this independent expert's report by Calkins was a range of theoretical works and in-flight investigations (undertaken, among others, by NASA) documenting the existence of threat to the safety of landing approach by such vortex (e.g. work by Nelson and Jumper "*Aircraft wake vortices and their affect on following aircraft*" [67]).

Published data shows that during the ten year period 1997-2006, 59% of fatal aircraft accidents were associated with *Loss-of-Control* (LOC) [77, 83, 103]. The notion of loss-of-control is not well-defined in terms suitable for

[1] Report NTSB [79]. Report stated, that a probable cause of the crash was the loss of control of the aeroplane (claimed in the original) „*The National Transportation Safety Board determines that the probable cause of the USAir flight 427 accident was a loss of control of the airplane resulting from the movement of the rudder surface to its blowdown limit. The rudder surface most likely deflected in a direction opposite to that commanded by the pilots as a result of a jam of the main rudder power control unit servo valve secondary slide to the servo valve housing offset from its neutral position and overtravel of the primary slide.*"

rigorous control systems analysis. The importance of LOC is emphasized in work [27] where the inadequacy of current definitions is also noted. On the other hand, flight trajectories have been successfully analyzed in terms of a set of five two-parameter envelopes to classify aircraft incidents as LOC [49]. As noted in that works, LOC is ordinarily associated with flight outside of the normal flight envelope, with nonlinear behaviors, and with an inability of the pilot to control the aircraft. These results provide a means for analyzing accident data to establish whether or not the accident should be classified as LOC. Moreover, they help identify when the initial upset occurred, and when control was lost. The analysis also suggests which variables were involved, thereby providing clues as to the underlying mechanism of upset. However, it does not provide direct links to the flight mechanics of the aircraft, so it cannot be used proactively to identify weaknesses or limitations in the aircraft or its control systems. Moreover, it does not explain how departures from controlled flight occur. In particular, we would like to know how environmental conditions (like icing) or faults (like a jammed surface or structural damage) impact the vulnerability of the aircraft to LOC. LOC is essentially connected to the nonlinearity of the flight control problem. Nonlinearity arises in two ways: 1) the intrinsic nonlinearity of the aircraft dynamics, and 2) through state and control constraints. In this paper we consider control issues that arise from both sources. First, we examine the implications of the nonlinear aircraft dynamics. Bifurcation analysis is used to study aircraft control properties and how they change with the flight condition and parameters of the aircraft.

The starting point, allowing to reconstruct an aircraft crash, is the data from many sources. The main source of information is the data coming from an on-board flight parameter recorder (for example SARPP-12). Apart from that, also recordings of conversations made by the crew, photos of the occurrence, drawings, witness statements, way and direction of scatter of the wreckage, after-crash investigations of the wreckage and other investigatory actions are taken into account.

This paper will discuss LOC in terms of controllability/observability, bifurcation analysis, and safe sets analysis in aspects of Theory of Catastrophe. The inter-relationships between these attributes and their relationship to aircraft LOC will be discussed. Investigating LOC requires the use of aircraft dynamical models that are accurate outside of the normal flight envelope. In particular it is necessary to characterize post stall and spin behaviors that are often associated with LOC events. We will specifically address control issues that arise near stall. We illustrate uncontrolled departures of generalized aircraft near stall (caused by icing for example) and give some first illustrations of recovery from post departure states. Additionally we consider difficulties associated with remaining within a specified flight envelope when control authority is limited. Finally we summarize our results in the cusp catastrophe terms.

2. Theory of Catastrophe - an overview

Catastrophes are bifurcations between different equilibriums, or fixed point attractors. It originates from the French mathematician Rene Thom in the 1960s. Thom has demonstrated through his classification theorem that all discontinuous phenomena that can be expressed in terms of four or fewer independent variables (also called control dimensions) which exit in many branches of science and these can be modeled using one of seven elementary catastrophes. The most commonly applied catastrophe has been the cusp model. Figure 1 shows the basic form of the generated deterministic cusp model.

Each catastrophe model can be formalized by potential or gradient structures, a potential function $F(\mathbf{x}, \boldsymbol{\mu})$ is a function of system state vector $\mathbf{x}$, and the control parameters vector $\boldsymbol{\mu}$. The Cusp Catastrophe Model consists of one behaviour variable and only two control variables. In works [60, 104] it is shown that the ability to regulate a system was lost at points associated with bifurcation of the trim equations; ordinarily indicating stall in an

aircraft. Such a bifurcation point is always associated with a degeneracy of the zero structure of the system linearization at the bifurcation point. As such points are approached; the ability to regulate degrades so that the performance of the regulator (or pilot) may deteriorate before the bifurcation point is actually reached.

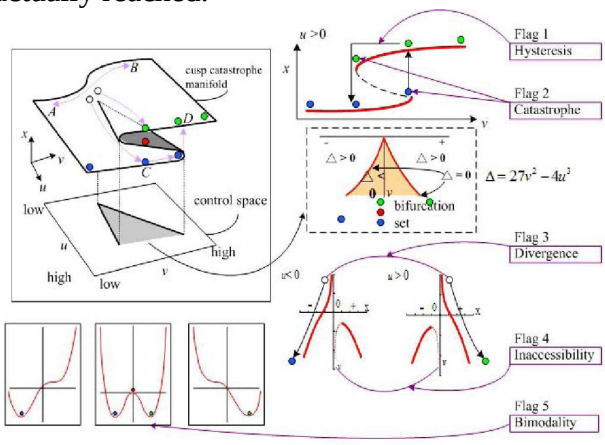

Fig. 1 A cusp catastrophe model

The equilibrium surface or set of trim conditions is a submanifold of the state-parameter space that is divided into open sets by the bifurcation points. Within each region a linear regulator can be designed. However, a regulator designed in one region will fail if applied in a neighboring region [103]. In the paper [45] Kwatny et all. we consider how state and control constraints relate to lost-of-control (LOC). In the paper [103] authors defined in-flight LOC as a *significant deviation of the aircraft from the intended flight path or operational envelope*. The flight envelope represents a set of state constraints, so it is possible to consider the control issues associated with preventing departure from the constraint set. It is possible to use the notion of a *safe set* [45] or *viable set* [44, 49]. Suppose an acceptable operating envelope is specified as a domain $\mathcal{C}$ in the state space. The safe set $\mathcal{S}$ is the largest positively control-invariant set contained in $\mathcal{C}$. Consequently, for any initial state in $\mathcal{S}$ there exists a control that keeps the trajectory within $\mathcal{S}$. On the other hand for an initial state in $\mathcal{C}$ it not in $\mathcal{S}$, there is no admissible control that will keep the trajectory in $\mathcal{C}$, the acceptable region. Thus, transitions out of $\mathcal{S}$ will require a restoration control that necessarily includes some period of time outside of $\mathcal{C}$. Above analysis is well described as cusp catastrophe (see Figure 1).

Human error is often cited as a major contributing factor or cause of incidents and accidents. Incident surveys in aviation have attributed 70% of incidents to crew error. Although a large portion of the accidents can be attributed to human error, many accidents are catalyzed by persons not present at the time of the event. In fact, it is this source of latent conditions that pose a most significant threat to the safety of complex systems. Another dimension to human errors that can precipitate the alignment or trigger the latent conditions. The risk associated with aviation is a dynamic element that is affected by both latent conditions and situational factors. This dynamic nature will be presented in the paper using the cusp model from catastrophe theory [76, 104]. Using Reason's [90, 81] latent failure model (Figure 2), the descriptive and predictive nature of the cusp catastrophe model works as a map to illustrate the nature of aviation accidents in terms of instability resulting from the alignment of latent conditions and influence of active errors.

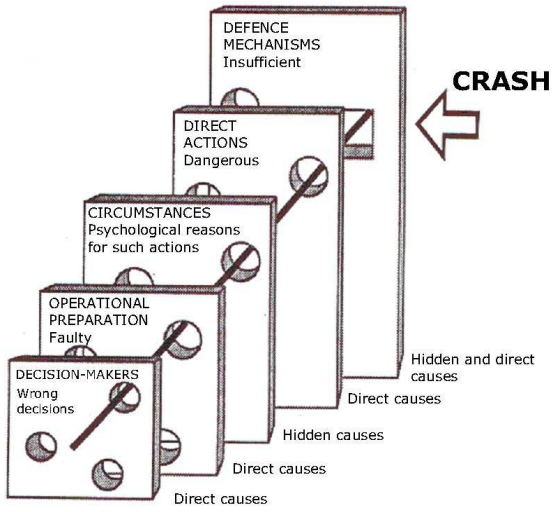

Fig. 2 Reason's model of occurrence of aviation catastrophe [80]

The dynamic nature of aviation and associated risks is a function of the situational factors and latent conditions present at the time. Both share a temporal a temporal and spatial element. Reason's latent failure model can be mapped onto the 3-D space of the cusp model (Figure 1), in order to illustrate the instability created when

active errors *v* and latent conditions *u* combine to place the point at the pleat, thereby leading to a catastrophe event. In this model, the active errors are contained as futures within the situational factors. Mistakes or errors within the catastrophe model will result in a move toward a more negative situational factor. These active errors may act as a trigger enabling the latent factors, thereby activating a series of effects or consequences with possible disastrous outcomes. The latent conditions are contained within systemic factors and range in value from low to high based on their emergence during a flight safety event. Point A represents a scenario characterized by positive situational factors and low systematic factors where the potential for flight safety incidents is very low. As the situation deteriorates the scenario develops a dynamic nature characterized as a movement along the axis *x* This situational factor triggers the latent (systematic) conditions characterized as a movement prom point A to point B in Figure 1. If uncorrected, a catastrophe event may occur beginning with the movement from point B to D where the instability of the situation results in the catastrophic event characterized by the movement from *D* to *C*. Similarly, situational factors may continue for sometime before triggering the latent conditions, as characterized as the movement from *A* to *D*. The complexity of the disaster aetiology stems from both the scale and coupling of the systems (not only the physical aircraft systems but also the organizational systems that support the operation). This complexity creates a pattern of disaster that evolves or is precipitated through a series of several small failures. The cusp catastrophe model facilitates the mapping of Reason's latent failure model, providing a descriptive and predictive illustration of the emergence of latent conditions under the trigger of situational factors. The risk of an accident increases as the situational and systematic factors combine to create an inherent instability resulting in the catastrophic event.

3. The Lost of Control Problem

Generally, a pilot will report LOC if the aircraft does not respond as expected. Consequently, pilot experience can be a major variable in assessing LOC. What LOC is to one pilot may not be to another. Wilborn and Foster paper [103] have proposed quantitative measures of LOC. These Quantitative Loss-of-Control (QLC) metrics consist of envelopes defined in two dimensional parameter spaces. Based on the analysis of data sets compiled by the Commercial Aircraft Safety Team (CAST) Joint Safety Analysis Team (JSAT) for LOC five envelopes have been defined [45, 77]:

1. *Adverse Aerodynamics Envelope*: (normalized) angle of attack vs. sideslip angle
2. *Unusual Attitude Envelope*: bank angle vs. pitch angle
3. *Structural Integrity Envelope* : normal load factor vs. normalized air speed
4. *Dynamic Pitch Control Envelope*: dynamic pitch attitude ($\theta + \dot{\theta}\,\Delta t$) vs. % pitch control command
5. *Dynamic Roll Control Envelope*: dynamic roll attitude ($\varphi + \dot{\varphi}\,\Delta t$) vs. % lateral control command

Kwatny et all. [45] provide a compelling discussion of why these envelopes are appropriate and useful. Flight trajectories from the 24 CAST data sets are plotted and the authors conclude maneuvers that exceed three or more envelopes can be classified as LOC, those that exceed two are borderline LOC and normal maneuvers rarely exceed one. According to [3], the precipitating events of the CAST LOC incidents were: stalls (45.8%), sideslip-induced rolls (25.0%), rolls from other causes (12.5%), pilot-induced oscillation (12.5%), and yaw (4.2%).

These results are important. They provide a means for analyzing accident data to establish whether or not the accident should be classified as LOC. Moreover, they help identify when the initial upset occurred, when control was lost and suggests which variables were involved. However, because the approach does not directly connect to the flight mechanics of the aircraft, it does not identify weaknesses or limitations in the aircraft or its control systems. Moreover, it does not explain how departures from controlled flight occur. In

particular, we would like to know how environmental conditions or actuator failures or structural damage impact the vulnerability of the aircraft to LOC. To do this we need a formal analytical definition of LOC.
Another important study [103] reviews 74 transport LOC accidents in the fifteen year period 1993-2007.
Of these the major underlying causes of LOC are identified as stalls, ice contaminated airfoils, spatial disorientation, and faulty recovery technique.
An aircraft must typically operate in multiple modes that have significantly different dynamics and control characteristics. For example, cruise and landing configurations. Within each mode there may be some parametric variation, such as weight or center of mass location, that also affects aircraft behavior. Each mode has associated with it a flight envelope restricting speed, attitude and other flight variables. Under normal conditions keeping within the flight envelope provides sufficient maneuverability to perform the mode mission while insuring structural integrity of the vehicle for all admissible parameter variations and all anticipated disturbances. Abnormal conditions, e.g., icing, faults or damage, will alter aircraft dynamics and may require the definition of a new mode with its own flight envelope.
Ordinarily a flight envelope can be considered a convex polyhedral set, not necessarily bounded, in the state space. Thus, the aircraft needs to operate within the state constraints imposed by the envelope. Insuring that an aircraft remains within its flight envelope is called *envelope protection*. Envelope protection is generally the responsibility of the pilot although there is an increasing interest in and use of automatic protection systems. Because the controls themselves as well as the states are constrained, the question of whether it is even possible to keep the aircraft within the envelope is not trivial. Questions like this have been considered in the control literature [7, 10, 22, 26, 27, 28, 45 - 48]. We will discuss the problem of identifying the largest set within a prescribed envelope which can be made positively invariant and of characterizing the control strategy necessary to do so. This set will be called the safe *set*. It is possible to be inside of the envelope and yet outside of the safe set. In which case it is impossible, no matter how clever the pilot or the control system, to keep the aircraft within its flight envelope. In a strict sense departure from the safe set implies LOC. It may, of course, be possible to employ a recovery strategy to restore the system to the safe set. So an aircraft may be out of control and yet recoverable. Besides the control bounds, other restrictions may be placed on the admissible controls that could further restrict the safe set. For instance, we could require that only smooth feedback controls be employed. These and related issues will be discussed below (see also [45]).

4. Bifurcation Analysis of Aircraft Dynamics

4.1. Dynamical systems theory (DST)

The transient and steady state of a system represented by a set of differential equations can be solved by conventional numerical integration methods, by computing the trajectories and orbits using digital simulation. However, it is possible with bifurcations theory to predict the behavior of trajectories and orbits without resorting to the solution of the differential equations. In this case, bifurcations analysis is applied to study the emergence of sudden changes in a system response arising from smooth, continuous variations on the system parameters. The results obtained with this analysis can be showed in a bifurcations diagram. The bifurcations diagram provides qualitative information about the behavior of the system steady state (equilibrium) solutions, as physical parameters are varied. At a certain points (bifurcations points) infinitesimal changes in system parameters can cause significant qualitative changes in equilibrium solutions. Broadly speaking, the construction of a bifurcation diagram consists of the following steps:

a) finding a first equilibrium solution of (1),
b) based on the first solution, find other equilibrium solutions based on a continuation method[20],

c) determining the stability of each solution. Each step is described next.

The system stability analysis based on the bifurcation approach requires of a set of differential and/or algebraic equations which contain two types of variables: states and parameters. In our case, the aircraft dynamic model is only characterized by a set of parameter dependent differential equations, that is:

$$\frac{d\mathbf{x}}{dt} = \mathrm{f}(\mathbf{x}, \boldsymbol{\mu}) \tag{1}$$

and

$$\mathbf{x} \mapsto \mathrm{g}(\mathbf{x}; \boldsymbol{\mu}) \tag{2}$$

with $\mathbf{x} \in U \subset \Re^n$,and $\boldsymbol{\mu} \in V \subset \Re^p$, where U and V are open sets in $\Re^n$ and $\Re^p$, respectively. We view the variables $\mathbf{x}$ as a vector of n state variables, the variables $\boldsymbol{\mu}$ as a vector of m parameters (or controls), $\dot{\mathbf{x}}$ is the time derivative of $\mathbf{x}$ and $\mathrm{f} : \Re^n \times \Re^m \to \Re^n$ is the smooth vector field (the n non-linear functions). Note that both open loop (uncontrolled) and closed loop rigid-body flight dynamical systems can usually be represented in the form of equation (1), and referred to [32] as a *vector field* or ordinary differential equation and to (2) as a *map* or *difference equation*. Both are termed *dynamical systems*.

By a solution of Eq. (1) we mean a map $\mathbf{x}$, from some interval $\Im \subset \Re^1$ into $\Re^n$, which we represent as follows

$$\begin{aligned} &\mathbf{x} : \Im \to \Re^1, \\ &t \mapsto \mathbf{x}(t) \end{aligned} \tag{3}$$

such that $\mathbf{x}(t)$ satisfies (1), i.e.,

$$\frac{d\mathbf{x}(t)}{dt} = \mathrm{f}(\mathbf{x}(t), t; \boldsymbol{\mu}(t)) \tag{4}$$

The starting point to the analysis of the aircraft dynamic model (1) is the identification of equilibrium points which define the equilibrium solution of the system under analysis. For an arbitrary fixed parameter μ_e, the equilibrium points $P_e=(x_e,\mu_e)$ are given by the values of and that satisfy the set of nonlinear algebraic equations given by once a first equilibrium solution has been computed, it is possible to know how the solutions of (2) vary with the increment of the system parameter in finite steps along a specified trajectory [32, 102]. At each step, the new equilibrium point is determined by the corresponding solution of (2) based on a continuation method [32]. A detailed mathematical description of this method can be found in [32]. Despite that the equilibrium solution obtained by solving (2) implies that the power system is at rest, this does not necessarily mean that the solution represents a stable operating condition [16, 29 - 31, 33 - 36]. The stability of the solution is determined by computing the equilibrium point's stability as described next. The principle of continuation is a mathematical technique in which the path of an established solution of a system of equations is followed around parameter space when a control parameter is varied [16]. The solution branch thus established can then be examined for special bifurcation points, at which a qualitative change of the preceding solution type can be observed. In dynamic systems, these qualitative changes frequently come in sequences: a stationary state is replaced by regular motion which can develop into irregular motion. The transition from regular to irregular motion is often related to the onset of chaos. Tracing the solution branches and detecting the bifurcation points, an accurate portrait can be drawn for the dynamics of the system. All continuation techniques are based on the fundamental assumption that the solutions of an ordinary differential equation (ODE) vary continuously with the initial conditions and the parameters of the ODE. Implementing a predictor–corrector scheme, a continuation algorithm can trace the path of an already established solution as the parameters are varied. This extrapolation appears to pull the solutions along an invisible path, thereby forming the corresponding solution branch. At intersections, where a solution generates two different solution branches, the algorithm can either resume continuation of the prevailing branch or perform branch switching to the intersecting branch.

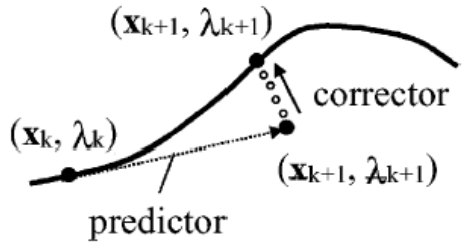

Fig. 3 Principle of arc-length continuation

Figure 3 illustrates the principle of arc-length continuation. Denoting the system parameter by and the *n*-dimensional state vector by a particular solution can be expressed by the – dimensional (1-D) vector. The index denotes the solution of the ongoing continuation process. The predictor determines a likely neighboring solution by linear extrapolation of the established solution branch in the direction of the tangent vector of the current solution. The predicted state is then corrected to the true solution using an iterative algorithm such as the gradient descending Newton–Raphson method (small circles in Figure 3). As this corrector is independent of the system dynamics, the continuation method is able to converge to solutions irrespective of their stability properties.

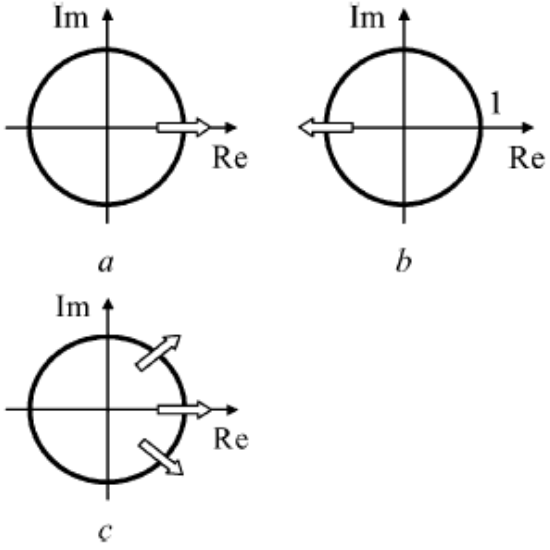

Fig. 4 Three scenarios of stability of a solution: (a) fold bifurcation, (b) flip bifurcation, (c) secondary Hopf bifurcation

The number of iterations required by the corrector can be used to adjust the step size of the predictor [34 - 36]. Loss of stability is encountered when a multiplier *leaves* the unit circle. This can occur in any of the following three ways (Figure 4). The methodology of continuation requires at least one solution of the system equations to be known. A suitably designed homotopy can be used to find this initial solution [30]. Alternatively, the dynamic equations can be integrated until the steady state has been reached. The continuation can thus be initiated with the set of state variables which result from a sufficiently long time-domain simulation. The stability of a limit cycle oscillations (LCOs) can be assessed from the corresponding characteristic multipliers or Floquet multipliers. These multipliers represent a generalization of the eigenvalues of an equilibrium point, as they describe the local contraction or expansion rate of phase space near the limit cycle of interest. Floquet theory is based on the observation that a periodic solution.

Solution can be represented through a fixed point of an associated Poincaré map [32, 34, 51, 53]. Consequently, the stability of an LCO can be determined by assessing the stability of the corresponding fixed point of this Poincaré map. Linearization of the Poincaré map at the fixed-point results in a linear discrete-time system which describes the period-to-period evolution of oscillations in the vicinity of the LCO. The Floquet multipliers are now given by the eigenvalues of the Jacobian of this linear system, the so-called monodromy matrix. Stable characteristic multipliers, being the eigenvalues of a map, are found inside the unit circle; conversely, unstable periodic limit cycles have at least one characteristic multiplier outside the unit circle. A *fold bifurcation* is encountered when a single real eigenvalues of the monodromy matrix crosses the unit circle at Figure 2a. The second scenario in which the stability of a solution can be lost is the *flip bifurcation* or *period-doubling bifurcation*. This case is given when a single real eigenvalue crosses the unit circle at Figure 4b. At this branching point, the prevailing solution branch becomes unstable and a new branch is born. Solutions on this new branch have twice the period of the previous limit cycle. In the frequency domain, this corresponds to the occurrence of a subharmonic at half the

previous frequency. The third possible loss of stability is through a Hopf bifurcation of the periodic solution (generalized Hopf bifurcation or torus bifurcation). This case is characterized by the crossing over the unit cycle of two complex conjugated eigenvalues and corresponds to the onset of quasiperiodic oscillations see Figure 4c.

The most important ideas of DST used in the paper will be introduced in the following sections. The first step in the DST approach is to calculate the steady states of the system and their stability. Steady states can be found by setting all time derivatives equal to zero and solving the resulting set of algebraic equations. The Hartman-Grobman theorem (p. 234 in reference [102]) proves that the local stability of a steady state can be determined by linearizing the equations of motion about the steady state and calculating the eigenvalues. The implicit function theorem (Ioos and Joseph [40], in Chap. 2) proves that the steady states of a system are continuous function of the parameters of the system at all steady states where the linearized system is non-singular. A singular linearized system is characterised by a zero eigenvalue. Thus, the steady states of the equations of motion for an aircraft are continuous functions of the control surface deflections and/or vector of the thrust inclinations. Stability changes can occur as the parameters of the system are varied in such a way that the real parts of one or more eigenvalues of the linearized system change sign. Changes in the stability of a steady state lead to qualitatively different responses for the system and are called bifurcations. Stability boundaries can be determined by searching for steady states, which have one or more eigenvalues with zero real parts. Continuation methods are a class of numerical algorithm used to follow a path of steady states in continuous or discrete dynamical systems as a parameter varies. They make use of the Implicit Function Theorem, which essentially states that if the Jacobian matrix **J** (5) of the system linearized at a stationary point is non-singular then this solution is *locally unique*, i.e. it is part of a unique curve of stationary points which is a continuous function of the parameters. The Jacobian matrix of an equilibrium point x_0 of a vector field or the fixed point x_0 is defined in Equation (5). The eigenvalues of the Jacobian matrix are important for the stability analysis. More information on DST can be found in the book of Wiggins [103].

$$\mathbf{J} = Df(x_0) = \begin{Bmatrix} \frac{\partial f_1}{\partial x_1} & \cdot & \cdot & \frac{\partial f_1}{\partial x_1} \\ \cdot & & & \cdot \\ \cdot & & & \cdot \\ \frac{\partial f_n}{\partial x_1} & \cdot & \cdot & \frac{\partial f_n}{\partial x_n} \end{Bmatrix} \tag{5}$$

Continuation methods rely upon the Implicit Function Theorem, which states that if the Jacobian of the linearised system at a fixed point is invertible (i.e. non-singular) then there exists locally a unique solution. So for all fixed points excluding those with a real eigenvalue lying at zero, there exists locally a unique fixed point for the given value of λ. Therefore for a smooth variation in λ from an initial fixed point there must exist a unique curve of fixed points (assuming that the Jacobian remains non-singular). As parameters vary in a dynamical system, changes may occur in the qualitative structure of the dynamics at certain parameter values. These changes are called bifurcations and the corresponding state/parameter values, bifurcation points. There are various types of bifurcations, classified according to the Centre Manifold and other dynamical systems theorems (see, for example [45]). The continuation algorithm solves for the branch using a predictor-corrector method. If an initial solution is known, then the system can be extrapolated in the local region by an incremental approximation in each system state Δx_i. Newton's method is then used to reduce the error between the approximation and the new fixed point. Most continuation methods possess the ability to solve through certain classes of singularity, e.g. folds. In order to generate all the branches that are present within a given parameter range, a complete set of starting solutions is required for the system. One of the main difficulties in applying bifurcation methods is finding these initial solutions. There are several approaches to solving this problem,

some systematic, some that require flight dynamics insight and some based on the nonlinear systems theory. It should be noted however that none of the methods can be guaranteed to find all the starting solutions for a given set of nonlinear equations. In most cases though, a combination of methods and perseverance allows a comprehensive set of starting solutions to be found. Starting with an approximation of a steady state for a given value of parameters, the computer code determines, by a continuation process, the solution curve $x(\mu)$ of a following set of non-linear algebraic equations, and determine type of bifurcation, (note: the continuation process assumes that all functions for (6) are continuous and have derivatives):

$$\begin{cases} \text{Equilibrium points} : & \mathrm{f}(\mathbf{x},\boldsymbol{\mu}) = 0 \\ \text{Limit points} : & \mathrm{f}(\mathbf{x},\boldsymbol{\mu}) = 0 \\ & \lambda = 0 \\ \text{Hopf points} : & \mathrm{f}(\mathbf{x},\boldsymbol{\mu}) = 0 \\ & \lambda_{1,2} = \pm 2i\pi / T \\ \text{Periodic orbits} : & x(T) = x(0) + \int_0^T \mathrm{f}(\mathbf{x},\boldsymbol{\mu})\,dt \end{cases} \tag{6}$$

As the branch is mapped out using a continuation algorithm, the system is linearised about each fixed point in order to investigate its local properties. The theorem attributed to Liapunov (1892) [40] relates the stability of a linearised system (with a non-singular matrix **A**) to the system eigenvalues λ_j of the Jacobian evaluated at the stationary point: $\mathrm{Re}(\lambda_j) < 0$ for all j implies asymptotic stability; $\mathrm{Re}(\lambda_k) > 0$ for one (or more) k implies instability of some kind. Two dimensional plots showing system state component solutions versus the continuation parameter usually created. The stability of each branch in these "one-parameter bifurcation diagrams" is typically indicated by line type. The conventions used in this paper are following: *Solid line* means stable all eigenvalues lie in the left half plane; *Dashed line* means unstable (divergent) one or more real eigenvalues lie in the right half plane; and *Dotted line* means unstable (oscillatory) only complex conjugate pairs of eigenvalues lie in the right half plane.

Since limit cycles are investigated here the only bifurcation results presented are those relating to system equilibriums, for which "divergent" and "oscillatory" unstable have equivalent meanings.

4.2. Continuation in the presence of control system saturation

With increasingly complicated control systems being developed, a continuation method that deals with this type of nonlinearity is highly desirable. Theoretically, if integrator wind-up protection were applied to this type of control system then steady states must exist even for regions of the flight envelope where saturation occurs. What would appear to be a continuous branch could be broken down into the saturated and non-saturated sections. (Note that a single control input has both a minimum and a maximum allowable position at which it saturates). The saturated section of the branch is directly analogous to carrying out a continuation with full deflection applied to one or more of the aircraft controls. The point at which the free system and the saturated system meet can be defined as a "break point".

Requirements for a suitable continuation method are:

1. it must be able to continue from one branch to the other at these break points
2. it must be able to cope with multiple control loops.

There are two possible approaches to this problem. The first is to identify the points at which the system saturates or desaturates and call different models when parts of the system saturate. This results in a piecewise continuation. Using a piecewise method allows the exact systems to be calculated and results in a rapid transition between the unsaturated and saturated regions. The second approach is to use an approximation to the saturation that allows the piecewise system to be modelled as a single continuous system. This means that no changes need to be made to the standard continuation software, for example XPPAUT [24], a WINDOWS® version of well known AUTO97 software.

4.3. Dynamic analysis using XPPAUT

A wide collection of useful numerical algorithms for the exploration of ordinary differential equations has been made available through the public domain software XPPAUT [24]. With its graphical interface to the popular continuation and bifurcation software AUTO, XPPAUT combines the advantages of two worlds: A set of ordinary differential equation can be integrated with the phase plane explorer XPP until a steady-state has been reached; once balanced, the system equations can then be passed to AUTO for continuation and bifurcation analysis. A convenient text-based interface allows the differential equations to be entered without the need for tedious low-level programming in FORTRAN or C. Figure 3 shows a screenshot of the main window of XPPAUT with the embedded AUTO in the foreground.

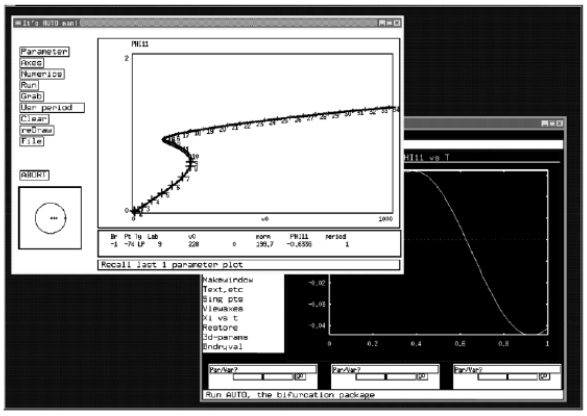

Fig. 5 Screenshot of the XPPAUT interface to AUTO

The problem definition file specifies a number of algorithmic options of XPP and AUTO. Noteworthy is the XPP option total which fixes the final time of the integration algorithm at one period (or). This parameter is read by AUTO to determine the period of the solutions to be continued. The option autovar= phi1 tells AUTO to use on the ordinate of the bifurcation diagram. Upon loading the above problem definition file into XPPAUT, an initial steady-state solution can be sought. The easiest way to achieve this is to use the boundary value problem solver of XPP; the relevant menus can be accessed using the mouse or via the key-stroke sequence. To improve the numerical stability of the iterations, the variable can be reset to 0 every time it reaches or exceeds. This cylindrical state space is defined using the sequence, followed by ENTER to accept the default maximum value of and the choice of as the variable to be restricted. Once a steady-state solution has been found, AUTO can be invoked through the key sequence. The AUTO window appears and should be made the active window. After having ensured that the ordinate shows the maximum value of the display variable, the continuation procedure can be started followed by a click on the OK button. As the continuation proceeds, the small area in the bottom left-hand corner of the AUTO window displays the evolution of the eigenvalues of the monodromy matrix. Loss of stability through any of the above scenarios can thus be directly observed. Notice that one of the three eigenvalues remains fixed. This particularity is inherent to the continuation of periodic solutions. The observed eigenvalue corresponds to translations of the system states in the direction of the trajectory of the associated Poincaré map. Subsequent states, which are found along this direction, exhibit a fixed distance. They are thus neither subject to compression (Floquet multiplier inside the unit circle) nor to expansion (Floquet multiplier outside the unit circle). Upon completion of the continuation step, the trace of a solution branch can be inspected for bifurcations and branching points. The menu item (G)rab allows navigation on a solution branch and reveals useful information of the established solutions. Various co-dimension-1 bifurcations such as limit points (fold bifurcation, denoted by LP), period doubling bifurcations (PD), and torus bifurcations (TR) can thus be identified with ease. Branching points at which the stability remains unchanged are labeled BP. Upon reaching a period doubling bifurcation (PD), the emerging branch can be continued. The direct visual feedback provided makes XPPAUT a powerful tool (e.g., convergence problems can easily be spotted (and remedied) as the continuation proceeds).

4.4. Nonlinear dynamics analysis methods of control system

Linear control design methods, which are used for the augmentation of aircraft dynamics,

usually do not take into account all of the important nonlinearities in the aircraft mathematical model. As a result, the handling qualities and stability characteristics may be satisfactory only at small disturbances from the controllable flight conditions. The qualitative analysis of aircraft closed-loop dynamics in such cases provides valuable information for control design. By varying free control-system parameters, like input interconnections, feedback gains, actuator constraints, etc., the closed-loop dynamics can be modified and improved, even for conditions where the applied control design method does not guarantee desired characteristics. The following computational methods for equilibriums and periodical orbits investigation, provided by the AUTO package, were used in this work for control law design:

1. continuation method along with the local stability analysis;
2. bifurcation-diagram method;
3. global stability analysis by computation of two-dimensional cross-sections of domain of attraction.

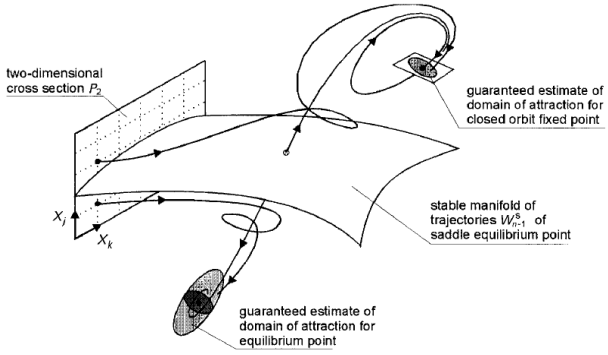

Fig. 6 Computation of two-dimensional cross-section of multi-dimensional domains of attraction (cf. [30]).

The continuation algorithm includes the orthogonal type of convergence to solution curves in the extended state space, thus improving bypass of aerodynamic kinks and turning points. It is also used in other algorithms of the AUTO package, such as the systematic search method for computation of multiple solutions of nonlinear systems, minimization of a functional under constraints defined by the nonlinear system, the boundary of stability region continuation, etc. This package also contains automatic routines for the systematic search for multiple solutions, their continuation with system parameters and the processing of bifurcation points. The direct method for investigation of multi-dimensional domains of attraction by computation of their two-dimensional cross-sections was outlined and applied for aircraft roll-coupling dynamics, where only the equilibrium states were considered. The proposed method can be applied in a similar way to the global stability analysis of an aircraft oscillatory motion.

Figure 6 provides the qualitative description of the method. In the multi-dimensional space of a dynamical system, formed from (1) and (2), the two-dimensional cross-section, P_2, is selected. For example, it can be defined by two vectors. One of the vectors gives the point belonging to the cross-section P_2, and the second assigns the normal vector to the plane. By the proper choice of orientation of the cross-section P_2, its coordinate system $(X_k;X_j)$ may coincide with any pair of state variables. The grid in the plane P_2 is defined depending on the required accuracy of stability region computation. The selected grid points provide initial conditions for numerical computation of dynamical system trajectories. Each attractor is surrounded by a special region, which is a subset of its full stability region. For example, this region can be estimated by means of the Liapunov function method. The entering of a state point inside this region defines the condition for termination of trajectory integration. Note that a closed orbit is represented by its fixed point and (n - 1) dimensional secant plane crossing a closed orbit in this fixed point. The total time for computation depends on the grid size and the sizes of the guaranteed estimates of all domains of attraction. Finally, this method provides the map in P_2 defining areas belonging to different domains of attraction. The outlined method is a very efficient tool, both for control law assessment and for control law design, because it permits identification of a very complicated topology structure of the stability region and gives accurate values for critical disturbances in the state variables.

Control-augmentation systems of modern aircraft involve both the direct interconnections between the control-surface deflections and different kinds of feedback. The direct

interconnections can significantly improve the controllability of an aircraft and avoid possible departures due to aircraft-motion coupling. The bifurcation diagrams in the plane of aileron, rudder or stabiliser deflections reveal the "departure-free" regions of the flight envelope. If interconnection keeps control surfaces inside the "departure-free" region, coordinated turns ($\beta = 0$) and departure prevention may be provided.

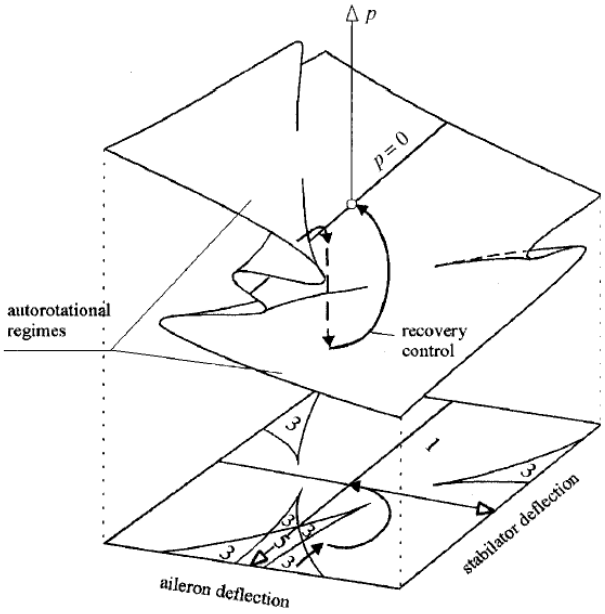

Fig. 7 Recovery control from critical autorotational regimes (cf. Goman, Kharamovsky [29] - illustration of cusp catastrophe).

Such interconnection at small control deflections is similar to well-known aileron rudder interconnection, used in many aircraft (Mehra [62]; Guicheteau [33 - 36]. The continuation technique can be applied to compute the nonlinear interconnection laws between stabilator, aileron and rudder, required to provide decoupling of longitudinal, directional and roll equilibrium states. Such decoupling may be useful during fast roll manoeuvres with strong aerodynamic and inertia interaction between longitudinal and lateral dynamics. When considering the roll-coupling problem, equation (1) is reduced to a fifth order system by neglecting the spiral motion, velocity change and gravity terms (Goman, Kharamovsky [29]). The equilibrium states will be defined by the following nonlinear system:

$$\mathrm{f}\left(\alpha,\beta,P,Q,R,\phi,\eta,\delta_a,\delta_r\right)=0,\qquad \mathrm{f}\in\Re^5 \tag{7}$$

Both state variables and control parameters in (7) are equivalent, therefore for continuation one can take the equilibrium states Q, R and control parameters ϕ, η, δ_a, δ_r as unknown variables, and the states α, β and P as some predefined parameters, say $\alpha = \alpha_{dem}$, $\beta = \beta_{dem}$ and $p = p_{dem}$.

In this case the nonlinear interconnections between stabilator, aileron and rudder will be computed by a continuation technique for every demanded manoeuvre α_{dem}, β_{dem} and p_{dem}.

Aircraft stability and control characteristics in spin and autorotational regimes may be very unusual for pilots, especially in comparison with common flight conditions. The determination of recovery control in flight dynamics simulation may be a very complicated problem due to motion coupling and reverse reaction on control inputs. To stop aircraft rotation and decrease aircraft incidence the problem can be formulated in terms of minimization of an "energy" like scalar function (Goman, Kharamovsky [29]),

$$W=\frac{1}{2}mV^2\left(\alpha^2+\beta^2\right)+\frac{1}{2}\left(J_X P^2+J_Y Q^2+J_Z R^2\right) \tag{8}$$

which defines the intensity of rotation and aircraft incidence (here m is aircraft mass, V is flight velocity, J_{xx}, J_{yy}, J_{zz} are aircraft moments of inertia in body axes). Recovery control can be determined as the minimization of the scalar function (8) considering aircraft equilibrium states

$$\min_u W\left(x\right),\quad \text{where } \left\{x\colon \mathrm{f}\left(x,u\right)=0\right\} \tag{9}$$

Application of a gradient descent method to the minimization problem of (9) gives the following differential form for the recovery control increment,

$$\mathrm{d}u=k\left[\frac{\partial W}{\partial x}\left(\frac{\partial \mathrm{f}}{\partial \mathrm{x}}\right)^{-1}\frac{\partial \mathrm{f}}{\partial u}-\frac{\partial W}{\partial u}\right] \tag{10}$$

An example of the recovery control computation is shown in figure 5 [29, 30]. The surface for equilibrium roll rate P and bifurcation diagram in the plane of stabilator δ_r, and aileron δ_a, deflections reveal the critical region with autorotational regimes the roll-coupling problem for low altitude and high velocity flight is considered). The recovery trajectory encounters the fold bifurcation on the

equilibriums surface and after the "jump" returns smoothly to the desired zero-rotation point.

5. Continuation methods – implementation to aircraft dynamics

The wide and purposeful applications of bifurcational methods and nonlinear dynamical system theory to flight dynamics nonlinear problem at high angles of attack regimes are now well-established [4 - 7, 10, 16, 18 - 20, 29 - 31, 33 - 36, 39, 41, 45 - 53, 52, 66, 86 - 93, 108].

The common feature of all these works is the implementation of the continuation technique for solving the nonlinear problems of an aircraft equation both for equilibrium and oscillatory motions. Carroll and mehra3 were the first who used the continuation method in flight dynamics and connected the main types of aircraft instabilities with bifurcation phenomena (e.g. The occurrence of wing rock motion was connected with a hopf bifurcation, the examples of chaotic motion were presented, etc). Later the existence of new types of bifurcations in aircraft dynamics were explored, e.g. Origination of stable torus manifold [30], global bifurcation of a closed orbit related with the appearance of homoclinical trajectory [29], so-called flip or period doubling and pitchfork bifurcations for closed orbits [29, 30] continuation methodology and bifurcation analysis can be used for determining the recovery technique from critical regimes and for control law design for improving dynamical behavior [51 - 53]. If the earliest works were devoted mainly to the theoretical methods and associated numerical procedures which can be used in aircraft dynamics [36, 41], the latest publications more often present the results of bifurcation analysis of high angle of attack dynamics of real aircraft (F-4 [16, 41], German-French Alpha-Jet [34], F-14 [16], F-15 [53]).

Comparisons between flight test results and predicted results obtained using bifurcation methods and numerical calculations for a number of aircraft show a very good agreement both in qualitative and quantitative senses. These comparisons reveal the efficiency and comprehension of bifurcational methods in flight dynamics applications. Therefore one can say that bifurcation methodology based on the computer-aided technology is becoming a popular and very powerful tool in the complicated nonlinear area of flight dynamics.

5.1. Bifurcation analysis and continuation technique methodology

Many characteristics, defining flight conditions, aircraft parameters and control surface deflections, can vary with time slowly. In many practical cases it is reasonable to consider such parameters as fixed ones and independent of time. This reduces the problem to a study of nonlinear autonomous dynamical systems. The system behavior in the case of parameter variations can be predicted using the knowledge about the specific system responses after encountering the bifurcation conditions**.**

Taking into account experience of many researchers, one can formulate the following three-step methodology scheme for the investigation of nonlinear aircraft behavior, the scheme being based on bifurcation analysis and continuation technique:

• During the first step it is supposed that all parameters (expect for the state variables) are fixed. The main goal is to search for all the possible equilibriums and closed orbits and to analyze their local stability. This study should be as thorough as possible. The implementation of the continuation technique to a great extent facilitates the solving of this problem. The global structure of the state space (or phase portrait) can be revealed after determining the asymptotic stability regions for all discovered attractors (stable equilibriums and closed orbits). An appropriate graphic representation plays an important role in the treating of the calculated and accumulated results.

• During the second step the system behaviour is predicted using the information about the evolution of the phase portrait with the parameters variation. The knowledge about the type of encountered bifurcation and current position with respect to the stability regions of other steady motions are helpful for the

prediction of further motion of the aircraft. The rates of parameter variations are also important for such a forecast. The faster the parameter change, the more the difference between steady-state solution and transient motion can be observed.

• Last, the numerical simulation is used for checking the obtained predictions and obtaining transient characteristics of system dynamics for large amplitude state variable disturbances and parameter variations.

5.2. The adequacy of a mathematical model

The adequacy of mathematical modeling of high angle-of-attack dynamics is strictly dependent on the adequacy of the aerodynamic model at these regimes. There is nontrivial problem due to the very complicated nature of the separated and vortex flow in unsteady conditions. Aerodynamics becomes extremely nonlinear and time history motion dependable. Qualitative and bifurcation approaches are also very fruitful when the sources and nature of aerodynamic phenomena are considered. Special techniques were proposed to represent the aerodynamic characteristics taking into account the dynamic effects of the separated flow [10, 25]. The bifurcation analysis of the jet aircraft was performed using the dynamical unsteady aerodynamic model at high angles of attack [1 - 3, 31, 106]. It is important to include the rotary balance data into the aerodynamic model in order to obtain better agreement with flight test results. The bifurcation methods of analysis of the nonlinear aircraft dynamics at high angles of attack can be efficiently used for validation of the aerodynamic models for these complicated flight regimes.

5.3. Autonomous forms of aircraft motion equations and steady state modes

There are some conventional forms of equations of motion which are commonly used in numerical and analytical studies of flight dynamics problems. If aircraft are considered as a rigid body three different frames of references are used to write the equations of motion, i.e. earth axes – $O_1x_1y_1z_1$ (inertial axes, flat approximation), body axes - $O_sx_sy_sz_s$ (axes fixed in a rigid body), wind-body axes – $O_ax_ay_az_a$ (origin is fixed in the mass center, O_ax_a is directed along the velocity vector V, and O_az_a lies in the plane of the symmetry of an airplane (see Figure 8).

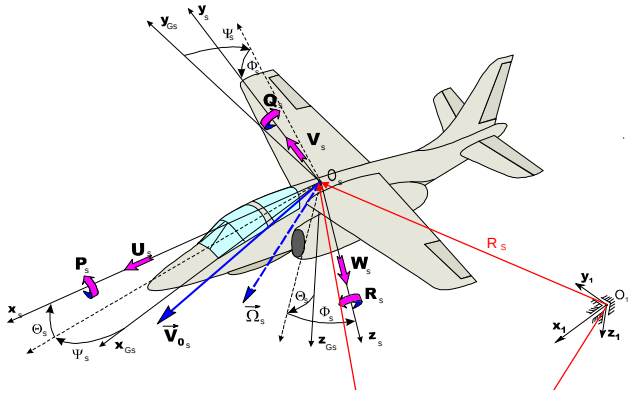

Figure 8 Inertial and rigid body axes

The full set of motion equations can be divided into the following four groups:

• Dynamics of translational motion written in wind-body axes:

$$\frac{dV}{dt} = \left(Tx_a - D - mg\sin\Theta_a\right)/m$$

$$\frac{d\alpha}{dt} = Q - \left(P\cos\alpha - R\sin\alpha\right)\tan\beta + \\ + \frac{Tz_a - L}{mV\cos\beta} + \frac{g}{V\cos\beta}\cos\Theta_a\cos\Phi_a \qquad (11)$$

$$\frac{d\beta}{dt} = P\sin\alpha - R\cos\alpha + \frac{Ty_a - C}{mV} + \\ + \frac{g}{V}\cos\Theta_a\sin\Phi_a$$

where (see figure 8):

$$\sin\Theta_a = -\cos\alpha\cos\beta\sin\Theta + \\ + \left(\sin\beta\sin\Phi + \sin\alpha\cos\beta\cos\Phi\right)\cos\Theta$$

$$\cos\Theta_a\cos\Phi_a = \sin\alpha\sin\Theta + \cos\alpha\cos\Theta\cos\Phi$$

$$\cos\Theta_a\sin\Phi_a = \cos\alpha\sin\beta\sin\Theta + \\ + \left(\cos\beta\sin\Phi - \sin\alpha\sin\beta\cos\Phi\right)\cos\Theta \qquad (12)$$

• Dynamics of angular motion written in principal body axes:

$$\frac{dP}{dt} = \left[\left(I_Y - I_Z\right)QR + \mathrm{L}\right]/I_X$$

$$\frac{dQ}{dt} = \left[\left(I_Z - I_X\right)RP + \mathrm{M}\right]/I_Y \qquad (13)$$

$$\frac{dR}{dt} = \left[\left(I_X - I_Y\right)PQ + \mathrm{N}\right]/I_Z$$

• Kinematics of angular motion written for wind-body axes (the same equation are valid for body axes without subscript (*a*):

$$\frac{d\Theta_a}{dt} = Q_a \cos\Phi_a - R_a \sin\Phi_a$$
$$\frac{d\Phi_a}{dt} = P_a + \left(Q_a \sin\Phi_a + R_a \cos\Phi_a\right)\tan\Theta_a \quad (14)$$
$$\frac{d\Psi_a}{dt} = \left(Q_a \sin\Phi_a + R_a \cos\Phi_a\right)\sec\Theta_a$$

• And kinematics of translational motion written in earth axes:

$$\frac{dx_1}{dt} = V\cos\Theta_a \cos\Psi_a$$
$$\frac{dy_1}{dt} = V\cos\Theta_a \sin\Psi_a \quad (15)$$
$$\frac{dz_1}{dt} = -V\sin\Theta_a$$

where altitude of flight H = ~ z_1.

The basic idea of the investigation of flight dynamics is the concept of steady states. The steady state of a flying vehicle is considered in a nonformal mathematical sense for a complete set of equations. Steady state or equilibrium is considered in a more general dynamical sense as the steadiness of all the external forces and moments, i.e. as the aerodynamic steady state. This condition requires that the main motion parameters (V, α, β, P, Q, R) and gravity projections (i.e. the Euler angles Θ, Φ) are all constant in the body axes frame with time. The position in space x_1, y_1 and head angle Ψ do not affect on the aerodynamic steady state, and therefore can be considered separately, together with appropriated equations. The altitude of flight H (or z_1) defines the air density and can be added to the system of equations only in cases when the influence of density variation on dynamics behavior is significant. If the variation of P with altitude can be neglected, the most general case of equilibrium flight is a vertical helicoidal trajectory. These may be climbing and gliding turns with large radius of curvature, or steady equilibrium spin modes with relatively small radius of trajectory curvature. The spatial case of such trajectories is the rectilinear motion. Therefore to study flight dynamics the following autonomous system of equations can be extracted from the full system (Eqs (l1)-(15))

$$\frac{d\mathbf{x}}{dt} = \mathrm{f}\left(\mathbf{x},\mathbf{u}\right) \quad (16)$$

where:

$$\mathbf{x} = \left[V,\alpha,\beta,P,Q,R,\Theta,\Phi\right]^T \in \Re^8, \text{ and}$$
$$\mathbf{u} = \left[\delta_e,\delta_a,\delta_r,T\right]^T \in \Re^4$$

are the state vector and the control vector. The steady state regimes, which are the vertical helicoidal trajectories, are defined by equilibrium solutions of this system of equations.

Some additional physical assumptions, concerning the type of motion, such as the existence of the plane of symmetry, steadiness of some state variables, etc., can be taken into account for obtaining the approximate autonomous subsystems of equation of lower dimension for investigation the flight dynamics. Such subsystems can be derived for symmetrical flight in vertical plane, for studying the roll-coupling problem, etc. (see the following sections).

5.4. Aerodynamic model for high angles of attack flight conditions

The aerodynamic model intended for spin conditions, i.e. high angles of attack and fast rotation, is based on the experimental data obtained from the different kinds of wind tunnel tests - static, forced-oscillation and rotary balance. There exist a number of methods for designing the “combined” mathematical model of aerodynamic coefficients, which implement the experimental data in a very similar manner [14, 18, 21, 27, 31, 42, 44, 56, 63, 65, 68, 70].

The rotation at high angle of attack can significantly influence the flow pattern. As a result, the aerodynamic coefficients become nonlinear functions of the reduced rate of rotation. That's why the aerodynamic coefficients measured in rotary balance tests are considered as the basic or “nondisturbed” part of the aerodynamic model for high angle-of-attack conditions.

The disturbed motion is accompanied by the misalignment between the velocity and the rotation vectors. The projections of the rotation vector onto the wind-body axes can be used as parameters for describing the disturbed conical

motion. The roll rate in wind-body axes $p_a = (p\cos\alpha + r\sin\alpha)\cos\beta + q\sin\beta$ defines the rate of conical rotation, which is similar to the angular rate in the rotary balance tests. Two other projections:

$$q_a = -(p\cos\alpha + r\sin\alpha)\sin\beta + q\cos\beta,$$

$$r_a = r\cos\alpha - p\sin\alpha$$

define both the unsteadiness and spirality of motion:

$$\dot{\alpha} = \left(q_a - q_{a_{sp}}\right)/\cos\beta,$$

$$\dot{\beta} = -r_a + r_{a_{sp}}$$

The values of $q_{a_{sp}}, r_{a_{sp}}$ are the wind-body angular rates in steady state spiral motion and their undimensional values $q_{a_{sp}}\bar{c}/2V$, $r_{a_{sp}}\bar{c}/2V$ are usually very small.

Assuming that the disturbances of the pure conical motion are small, the following representation of the aerodynamic coefficients can be used:

$$\begin{aligned} C_i &= C_{i_{RB}}(\alpha,\beta,p_a,\mathbf{u}) + C_{i_{q_a}}\frac{q_a\bar{c}}{2V} + \\ &+ C_{i_{\dot{\alpha}}}\frac{\dot{\alpha}\bar{c}}{2V} + C_{i_{r_a}}\frac{r_a b}{2V} + C_{i_{\dot{\beta}}}\frac{\dot{\beta}b}{2V} \\ &= C_{i_{RB}}(\alpha,\beta,p_a,\mathbf{u}) + \left(C_{i_{q_a}} + C_{i_{\dot{\alpha}}}/\cos\beta\right)\frac{q_a\bar{c}}{2V} + \\ &+ \left(C_{i_{r_a}} + C_{i_{\dot{\beta}}}\right)\frac{r_a b}{2V} - C_{i_{\dot{\alpha}}}\frac{q_{a_{sp}}\bar{c}}{2C\cos\beta} + C_{i_{\dot{\beta}}}\frac{r_{a_{sp}}b}{2V} \end{aligned} \tag{17}$$

The derivatives of the aerodynamic coefficients, standing together with the reduced rates of rotation and corresponding to the rotary flow, can be measured, by means of the oscillatory coning technique, such as already in use at ONERA/IMFL [98]. The terms with $q_{a_{sp}}$ and $r_{a_{sp}}$ can be omitted.

In many cases the data obtained from "traditional|" forced oscillations tests (recall that they measured in the absence of the model rotation) are used. The following approximate transformation, which is valid for zero sideslope, may be used:

$$\begin{aligned} C_{i_{q_a}} + C_{i_{\dot{\beta}}} &\simeq C_{i_{q_a}} \\ C_{i_{r_a}} - C_{i_{\dot{\beta}}} &\simeq C_{i_{r_{fo}}}\cos\alpha_0 - C_{i_{r_{fo}}}\sin\alpha_0 \end{aligned} \tag{18}$$

where the subscript "fo" denotes the data obtained in forced oscillation tests.

When the nonlinear term in (17) can be approximated by a linear function on the angular rate, the representation (17) becomes equivalent to the aerodynamic model commonly used for low angles of attack. The results of the static wind tunnel tests in this case can also be incorporated into the mathematical model.

The form of the aerodynamic model (17) for stall/spin conditions is quite natural. For example, the rotary derivatives $C_{i_{q_a}}$ and $C_{i_{r_a}}$ do not significantly affect either the values of kinematic parameters at the equilibrium spin or their mean values during the oscillations with moderate amplitude. These derivatives as well as unsteady derivatives $C_{i_{\dot{\alpha}}}$ and $C_{i_{\dot{\beta}}}$ directly affect on the stability margin of the oscillatory spin mode. Thus they determine, for example, the amplitude of the 'agitated' spin motion, when the equilibrium spin is oscillatory unstable.

The rotary balance data $C_{i_{RB}}(\alpha,\beta,p_a b/2V,\mathbf{u})$ in the aerodynamic model allows getting realistic values of the equilibrium spin parameters. To improve the time histories and amplitudes of the oscillations, one can make some adjustments (if necessary) to rotary and unsteady derivatives $C_{i_{q_a}}, C_{i_{r_a}}, C_{i_{\dot{\alpha}}}, C_{i_{\dot{\beta}}}$. All the wind tunnel data are measured and tabulated in a wide state and control parameter ranges. To facilitate the implementation of the continuation technique the aerodynamic functions are usually smoothed by means of spline or polynomial approximation to ensure continuity and derivability conditions for the resulting nonlinear dynamic system.

Aerodynamic asymmetry is one of the important features of aerodynamic coefficients at high angles of attack. Asymmetry appears at zero sideslip, rate of rotation and symmetrical aileron and rudder deflections. It may be larger than maximum aileron and rudder efficiency. Asymmetrical roll moment can significantly influence stall behavior; asymmetrical yaw moment arises at the higher angle of attack

region and to a great degree defines the spin dynamics. Due to asymmetry, the right spin modes can greatly differ from the left ones both in the values of parameters and the character of stability.

Unsteady aerodynamic effects at high angles of attack, resulting from the separated and vortex flow development, can significantly transform the real aerodynamic loads with respect to their conventional representation, which was discussed above. In the frame of the conventional approach the unsteady effects are described using linear terms with unsteady aerodynamic derivatives. There are special regions of incidence, e.g. C_{Lmax} region, where the conventional representation is not valid. The special approaches using the differential equations or transfer functions can improve the aerodynamic model and take into account the nonlinear unsteady aerodynamic effects due to separated and vortex flow dynamics.

5.5. Aircraft with control augmentation system [4]

Modern airplanes are equipped with automatical control systems able to change its dynamical properties radically. Aircraft with flight control systems become more nonlinear and higher dimensional plant. In addition, a flight control system introduces further nonlinearity and additional dynamic elements. Even in the case where an aircraft may be represented as a linear system, there will be appreciable nonlinearity due to actuator rate and deflection limits. The nonlinear behavior will be displayed during large amplitude motion at large control inputs or gust disturbances.

Nonlinear stability and bifurcational analysis methods also can be implemented for aircraft closed-loop system. The equations governing the operating of the control system can be added to the aircraft Eq. (16):

$$\frac{d\mathbf{u}}{dt} = \mathrm{g}\left(\mathbf{x}, \frac{d\mathbf{x}}{dt}, \mathbf{u}, \mathbf{s}\right) \qquad (19)$$

where $\mathbf{s} = [x_e, x_a, x_r, x_T]^T$ is a vector of the stick, rudder pedal, and throttle deflections The vector-function g is determined by the control laws and control system constraints.

Thus, for example, the following joint system is to be used for determining the equilibrium regimes of the aircraft:

$$\begin{matrix} \mathrm{f}(\mathbf{x},\mathbf{u}) = 0 \\ \mathrm{g}(\mathbf{x},\mathbf{u},\mathbf{s}) \end{matrix} \qquad (20)$$

The elements of the vectors **x** and **u** are the unknowns, and vector **s** defines the set of control parameters.

The specific features of Eqs. (19) and (20) are the limits on the values of some state variables (i.e. the deflections of the control surfaces

$$\mathbf{u}: \left(\delta_{e_{\min}} < \delta_e \le \delta_{e_{\max}}; |\delta_a| \le \delta_{a_{\max}}; |\delta_r| \le \delta_{r_{\max}}\right).$$

In nonlinear system with such state variable limits some additional equilibrium solutions can arise with associated limit points bifurcations leading to aircraft departures.

The maneuvering capabilities of the airplane are usually limited by some boundary. Outside this boundary lies the area of critical flight regimes, i.e. the regimes when uncontrollable motions (connected with the loss of stability) develop. Pilots' actions may either provoke or prevent the development of the instability. It depends on the task being performed and on the pilot's skill in flying the plane in such regimes [4].

A desire to enhance maneuverability inevitably results in entering the regions, where aerodynamic characteristics are nonlinear and dynamic cross-coupling between different forms of motion cannot be ignored. As a result, the dynamical problems become highly nonlinear. All the critical regimes can be divided into two groups, according to the reasons of dangerous behavior of the vehicle.

The regimes of the first group arise when the stability margin is broken and the unstable modes of motion begin to develop. These regimes are very different. There may be mild or abrupt loss of stability, and the motion may be controllable or uncontrollable. Such situations take place during stall or maneuvers with fast roll rotation.

The second group comprises the stable steady-state flight regimes with supercritical values of parameters (especially angle of attack and rate of rotation). The roll-inertia rotation or autorotation rolling and spin regimes belong to this group; the unusual response to the control

inputs is their characteristic feature. Departure resistance to the entering in these critical regimes and the methods of recovery from them are the most important questions, when the problem of flight safety is considered (see Fig. 7).

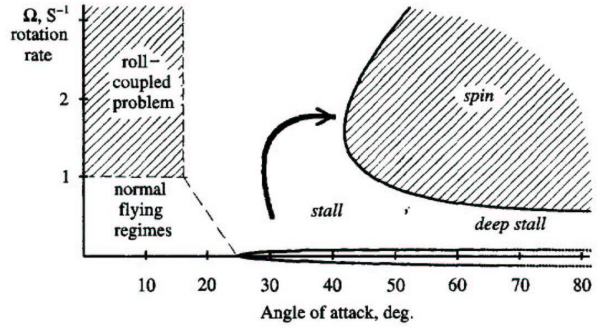

Figure 9 Critical flight regimes regions.

A number of different forms of the loss of stability in longitudinal and lateral/directional motion is usually connected with aircraft stall concept[56] . One may distinguish among them:

- a sudden rise of the angle of attack ("pitch up") taking place at moderate and high angles of attack due to pitching moment nonlinearity;
- stable self-oscillating pitching motion at high angles of attack due to the development of the separated flow ("bucking");
- the full turn rotation in pitch ("tumbling");
- divergent increase in the bank angle ("wing drop" or "roll off") due to asymmetrical aerodynamic rolling moment at high angle of attack or propelling aerodynamic moments;
- divergent increase in sideslip angle ("nose slice" or "yaw off") due to aperiodic instability in yaw or asymmetric aerodynamic moments;
- oscillating motion in roll and yaw at high angles of attack ("wing rock"');
- loss of stability due to the pilot's actions, for example, when the attitude stabilization or target tracking is performed.

There are also terms used in the flight dynamics for describing the aircraft behavior after stall, i.e. post-stall gyration, spin and deep stall. The post-stall gyration is a transient rotational motion of aircraft to the developed spin mode. The developed spin can possess very different features. It can be steady with constant parameters or "agitated", flat or steep, erected or inverted. "Agitated" spin mode can be with regular and "irregular" oscillations. Deep stall is an aircraft equilibrium flight at high critical angle of attack without rotation.

The possibility of the loss of stability and controllability at high roll rate (roll-coupled problem) is also well-known. This phenomenon is especially dangerous for supersonic aircraft with elongated ellipsoid of inertia and high level of lateral aerodynamic stability, which bring about cross-coupling of longitudinal and lateral motions. Roll-inertia rotation or autorotation rolling of the airplane (the trajectory being approximately horizontal and angles of incidence below stalling) is similar to the developed spin modes. The rotation can occur despite neutral or anti-rotation aileron and rudder deflections.

In both cases there are autorotational regimes, the difference is only in the nature of the aerodynamic moment that supports the rotation. All types of motion mentioned above can be connected with qualitative features of motion equations, i.e. the different steady-state aircraft motions and bifurcations, changing their stability conditions.

5.6. Analysis of the longitudinal motion

As was mentioned above the interaction between the phugoid and angular modes is more significant for flight with low velocities. In this case the large variation of angle of attack can arise due to trajectory distortion. For example, such trajectory distortion accompanies the tail-slide maneuvers.

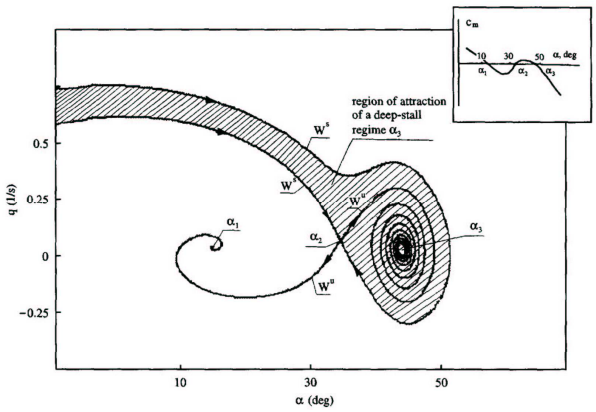

Figure 10 Phase portrait for the deep stall nonlinear dynamics.

The region of attraction of critical deep stall

regime in the general case will be more complicated with respect to the region, considered above in simplified manner. To take into account the interaction between phugoid and angular modes the first four equation of (20), which are the autonomous nonlinear system with state vector $\mathbf{x}=[V,\Theta,\alpha, q]^T$, have to be considered with entire ranges of α and Θ variations $[-\pi, \pi]$. To represent the stability region in the fourth-order state space it is possible only by means of drawing its two-dimensional cross-sections considering the disturbances only in two selected state variables.

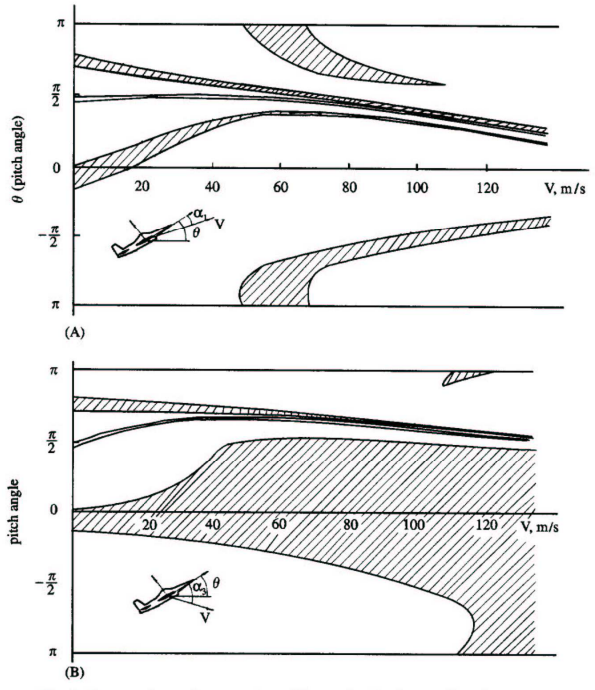

Figure 11 Crss section of asymptotic stability region for deep stall regime α_3 (cf. ref. [30])

For example, in Figure 9 two different cross-sections of the region of attraction of deep stall regime, i.e. stable point α_3, are shown. The disturbances in the plane of pitch angle Θ and velocity V are considered. Two other state variables at the initial moment are the same for all points of cross-section. In the first case (A) the angle of attack is trimmed in a lower stable point $\alpha = \alpha_1$ with zero pitch rate $q = 0$, and in the second case (B) the angle of attack is trimmed in the critical position $\alpha = \alpha_3$, also with zero pitch rate $q = 0$. In every point of the considered cross sections the initial path angle can be calculated using the following formula $\gamma = \Theta - \alpha$. The dashed areas on the cross sections define the initial points, starting from when the aircraft enters in the deep stall regime, α_3. In the second case (B) the probability of entering into the deep stall is much greater, especially in flights with large velocities, than in the first case (A). The number of cross sections of multidimensional stability region can offer global information about the aircraft dynamics.

The main feature of the problem considered is that even in the case of linear representation of aerodynamic coefficients the existence of multiple stable steady-state solutions, e.g. equilibrium and periodic, is possible. The bifurcational analysis of all the possible steady-state solutions and their local and global stability analysis can show the genesis of stability loss and explain in many cases the very strange aircraft behavior.

The validity of the system (16), (19) is confined in time. Therefore, in the cases of weakness or lack of stability of the steady states the conclusions resulting from the consideration of the asymptotic stability in Liapunov sense, when $t \to \infty$, can be wrong. A similar problem can arise for short-term control inputs. The prediction of the bifurcation analysis will be more consistent when the considered steady states have the sufficient margin of asymptotic stability. In any case the numerical simulation of aircraft motion using the complete set of equations has to be used for final verification of the bifurcational analysis results.

5.7. Bifurcational analysis of roll-coupling phenomenon

To demonstrate the possibilities of bifurcational and global stability analysis when roll-coupling problem is studied, two different examples will be considered. The first one is taken from Ref. 21 (pp. 447-451) and corresponds to a small maneuverable single-engine jet airplane at flight with zero altitude $H = 0$ and subsonic velocity V = 250 m/s. The second one corresponds to hypothetical swept-wing fighter at flight with altitude H=20000 m and supersonic velocity V = 750 m/s. The types of equilibrium solutions in these cases are different due to various contributions of damping terms in motion equations.

In the first case (H = 0, V = 250 m/s) all the

equilibrium solutions form the single continuous surface. The equilibrium surface in this case possesses the canonical form of a singularity in the mapping of the equilibrium surface on the plane of control parameters δ_e, δ_a, which are called "cusp catastrophe" and "butterfly catastrophe". Although the catastrophe theory was developed for the gradient type of dynamical systems, the formulated singularities are, nonetheless, also apparent in the autonomous dynamical systems.

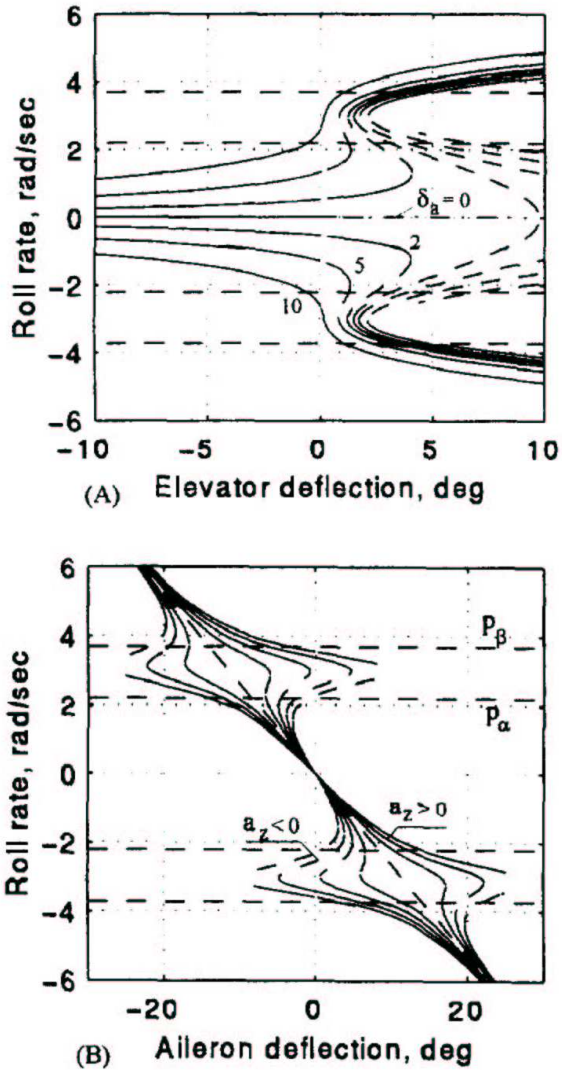

Figure 12 Equilibrium roll rates for different elevator and aileron deflection A) δ_e var, δ_a=0; B) δ_a var, $a_z = -0.4 \div 3.0$ [cf. [30])

In Fig. 12 the common view of the calculated equilibrium surface is shown along with the bifurcational diagram below it in the plane of elevator and aileron deflections. The number of equilibrium solutions, shown in the figure, varies with control inputs. There is a critical region with auto-rotational rolling regimes at pitch-down elevator and near-neutral aileron deflections ("butterfly catastrophe"). At pitch-up-elevator deflections there are two "cusp catastrophes", which lead to the hysteresis type behavior under the roll control. The quantified dependencies of equilibrium roll rate p on the aileron for a number of elevator deflections, corresponding to different initial values of normal factor $a_z \in (-4,3)$, are presented in Figure 11b. Another set of such dependencies on elevator deflections for δ_a var. is presented in Figure 12A (solid lines—stable solutions, dashed lines—divergent solutions, dash-dotted lines—oscillatory unstable solution). The approximate Phillips' critical roll rates $p_a = \sqrt{-m_2/i_q}$; $p_\beta = \sqrt{n_\beta/i_r}$ obtained without taking into account the damping terms, nevertheless define the roll-rate regions where the roll-coupling effect is more significant. These critical roll-rate values are shown in Fig. 10B by horizontal dashed lines. The oblique dashed line defines the controllability in roll mode without taking into account the dihedral roll moment, arising due to the inertia coupling of longitudinal and lateral motions.

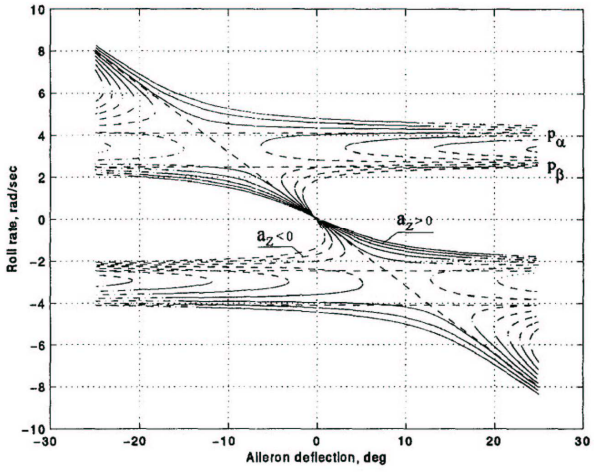

Figure 13. Equilibrium roll rates as a function of aileron deflection for initial trimmed flight with a_z = -2 ÷ 5[6].

In the second case (H = 20000 m, V= 750 m/s) the critical roll rates really exist and are very close to Phillips' approximate values. As a result the equilibrium solutions are divided by this critical line into different unconnected

families, which are shown in Figure 13. The dependencies of equilibrium roll rate on aileron deflection are presented for different elevator deflections, corresponding to different values of normal factor parameter a_z = -2 ÷ 5. As in the previous case the type of line defines the code of equilibrium stability (solid lines - stable solutions, dashed lines -divergent solutions, dash-dotted lines - oscillatory unstable solutions).

There are two different subcritical types of curves starting from the zero point. The first ones for positive a_z > 0 possess the "loss of controllability" - the increase of control moment does not proportionately increase the roll rate. This effect is due to the arising of opposite roll moments from sideslip, resulting from roll coupling. The second ones for zero and negative $a_z \leq 0$ possess the departure point, where stable and divergent equilibriums disappear.

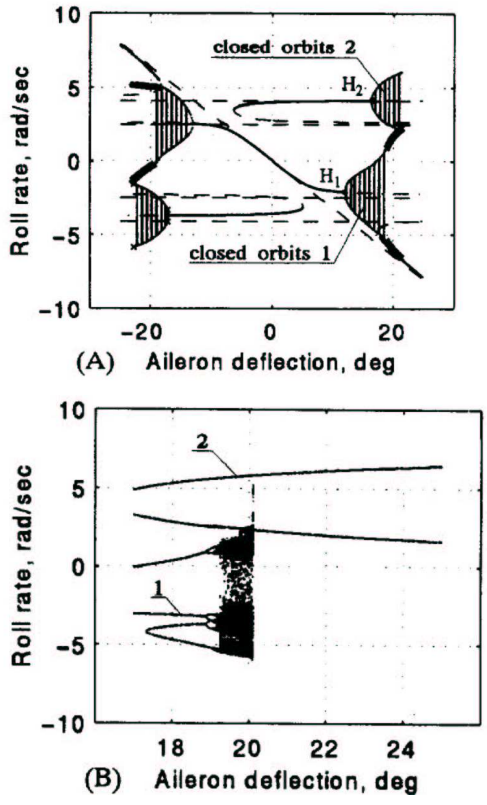

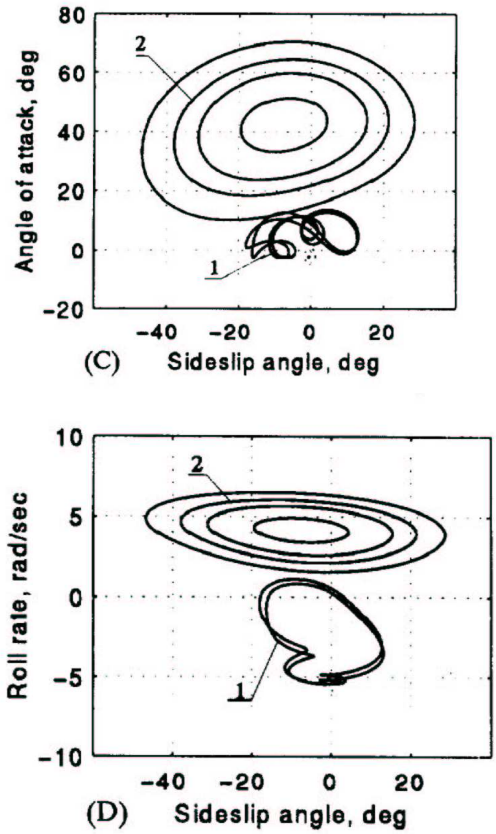

Figure 14 Periodical and chaotic behavior at fast-roll maneuver.

There is also another family of equilibrium curves both between the critical rates px, pp and in the outer regions. Some of them, corresponding to a_z = 1, 0, -1, - 2, generate the stable autorotational rolling regimes at zero aileron deflection. The autorotational rolling solutions for a_z = 0, -1, -2 exist at all aileron deflections, but at "pro-roll" aileron deflections (p > 0, δ_a> 0) the autorotational equilibrium solutions become oscillatory unstable (dash-dotted lines) and after the Hopf bifurcation point on each curve the family of stable closed orbits arises. A similar oscillatory instability of equilibrium solutions appear at subcritical equilibrium curves at large aileron deflections. The Hopf bifurcation points in this case also give birth to the families of stable closed orbits. To illustrate this in Fig. 14A the different branches of the equilibrium curves and the families of closed orbits placed on the subcritical and supercritical equilibrium branches for case with δ_e =-5.4° (a_z = 1.0) are presented.

The envelope curves denning the maximum and minimum values of roll rate in oscillatory

solutions at $\delta_a > 0$ pass through the Hopf bifurcation points H_1 and H_2. The oscillatory solutions originating in the point H_2 are stable at all values of aileron deflections. But the oscillatory solutions originating in the point H_1 on subcritical equilibrium branch become unstable at $\delta_a \approx 18.9°$. After this the cascade of flip or period-doubling bifurcation leads to the appearance of chaotic motion.
The bifurcation tree for the closed orbits originating in point H: was obtained by numerical Poincare mapping with the cross section plane $\beta = 0$ for different aileron deflections. It clearly shows the chaotic motion appearance (see Figure 14B). The amplitudes of the state variables in the stable oscillation regimes can be seen in bottom of Figure 14C, D, where the (α, β)- and (p, β) projections of the closed orbits for different aileron deflections are presented.

6. Case studies

The fatal aircraft accidents described below show an accidents aetiology that reflect Reason's latent failure model. Situational factors such as malfunction of engine bearing system, to high airspeed (over the tailplane flutter boundary), loss of space orientation caused by malfunction in longitudinal control system or fatal weather conditions with great probability of icing forced the pilots to be reliant on the standby instruments for at least some portion of the last minutes of the flight. Latent (systemic) factors that can be constructed to be contributing factors include the following:

- Aircraft certification standards for bearings manufacturing technology and turbine strength chain (too high overload factor turbine blades) (IL-62),
- Aircraft certification standards for material flammability were inadequate in that allowed the use of materials that could be ignited and sustain or propagate fire caused by hot parts of aircraft engine turbine penetrating the tail part of fuselage (IL-62),
- There were no built-in smoke and fire detection and suppression devices in the area where the fire started and propagated, nor were they required by regulation. The lack of such devices delayed the identification of the existence of fire in the aft part of fuselage, and allowed the fire to propagate unchecked until it became uncontrollable. The fire caused significant reduction of aft part of fuselage, and sudden relocation of passengers to the front of airliner (IL-62),
- Flight planning and managing error, (the yet training aircraft catastrophe),
- The lost of space orientation caused by malfunction in longitudinal control system, and lack of outside visual references forced the pilot to be reliant on the standby instruments for at last some portion of the last minutes of the flight. In the deteriorating cockpit environment, the positioning and small size of these instruments would have made it difficult for the pilots to transition to their use, and to continue to maintain the proper spatial orientation of the aircraft (The MiG 21bis fighter aircraft catastrophe),
- fatal weather conditions\, and management errors (TS-11 yet trainer catastrophe).

6.1. The of IL-62 airliners fatal accidents [58]

An example that reflect Reason's latent failure model can be the reconstruction of the tragic flights of the Il-62 “Kopernik” airliner, which happened on March the 14th 1980 near Warsaw Airport, and the Ił-62M “Tadeusz Kościuszko” airliner, which happened on May the 9th 1987[27]. As a result of laboratory research it was determined, that the cause of the crash was the destruction of left inner engine as a result of fault in manufacturing process or the low pressure turbine shaft. As a result, a crack of the shaft occurred, and the mechanic link between the turbine and the compressor was broken. Whole power of the turbine during several dozen milliseconds was used to increasing its rotation velocity, to the value at which the strength of the toothed ring of the turbine was lower than the occurring strains caused by the forces of inertia. A burst of the turbine toothed ring occurred. Splinters completely destroyed the system of control of the elevator. As result uncontrollable aeroplane hit the ground, and over 120 people died. Figure

1 shows the results of numerical reconstruction of flight trajectory.

Similarly, the second accident was caused by the destruction of left inner engine as a result of burst of toothed ring of low pressure turbine. This occurred as a result of a break of the shaft of this turbine, caused by a malfunction of a bearing. During this tragic flight the use of the bearing got into a critical state, which caused the seizure of labyrinth seals rotating in relation to the sleeve. As a result emission of a lot of heat occurred, the shaft of the turbine heated up to a temperature, in which its strength dropped below permissible value. A crack of the shaft occurred, and the mechanic link between the turbine and the compressor was broken. Whole power of the turbine during several dozen milliseconds was used to increasing its rotation velocity, to the value at which the strength of the toothed ring of the turbine was lower than the occurring strains caused by the forces of inertia. A burst of the turbine toothed ring occurred. Splinters destroyed the system of control of the elevator, and caused a fire in the luggage compartment. In the final phase of flight fire destroyed the trimmer of the elevator control system. Uncontrollable aeroplane hit the ground. As a result of this crash 187 people died.

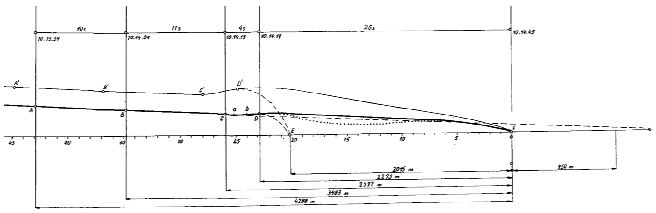

Fig. 15 Reconstruction of flight trajectory of the Il-62 "Kopernik" aircraft on March the 14th 1980 near Warsaw Airport Okecie

Work[27] contains not only a digital reconstruction of this flight, but also an attempt to answer the question whether the "Tadeusz Kościuszko" airliner could have landed on the runway of Okęcie airport, if the trimmer control system was not destroyed in the last phase of flight. Research showed, that this is a highly dangerous situation and probability of success practically equals zero.

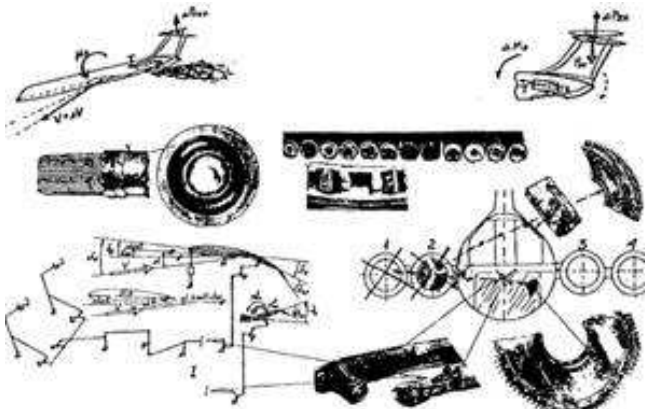

Fig. 16 Schematic explanation of this catastrophe case

6.2. The crash of the "W-300" prototype aircraft, near Radom, (January 30th 1987)

Particularly dangerous dynamic states of flight can be caused by deformability of structure, which applies mostly to the rear part of the fuselage and horizontal control surfaces. This structural defect can cause a pull into dive and, with brutal controlling, can lead to the destruction of control surfaces, and lead the aeroplane into an autorotation roll with very large negative gravity loads.

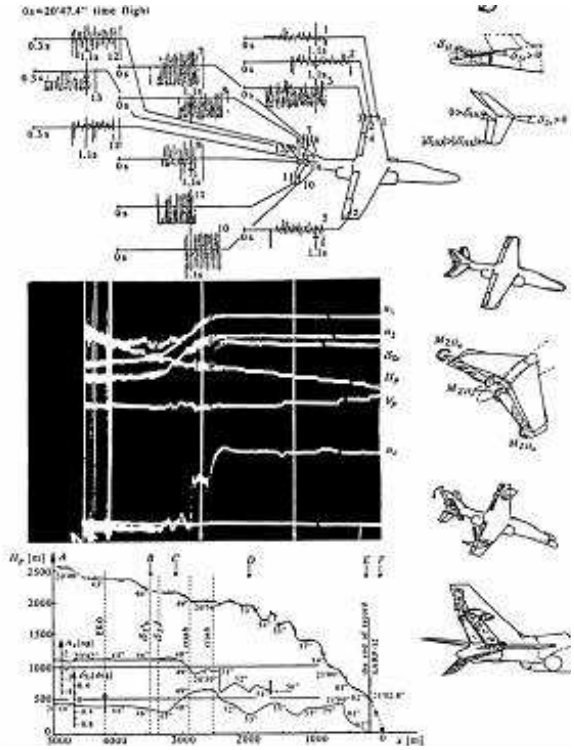

Fig. 17 Crash of the prototype "Iryda" aircraft, Radom, January 1987 – record of parameters of SARPP 12 recorder, results of numerical simulation and hypothesis of accident – tail plane flutter [57]

An example illustrating possibility and purposefulness of the use of simulation methods for reconstructing flight path of aircraft crashed is a successful attempt of recreating a crash of "W-300" Iryda prototype aeroplane, which took place near Radom January the 30th 1987. A direct cause of this crash was damage of the horizontal stabilizer, caused by excessive deformability of a part of the tail beam, which as a consequence lead to occurrence of flatter of control surfaces.
The crash was reconstructed on the basis of automatic record of recording device SARPP-12. The record of the last three seconds of that fatal flight is presented in Fig. 17.

6.3. Fatal crash of the MiG-21 bis aircraft (June the 28th 1996)

Another example of accidents aetiology that reflect Reason's latent failure model fatal accident of the MiG-21bis fighter aircraft, which took place on June the 28th 1996. Analysis of record of the recorder allowed the division of this tragic flight into three stages: stage "A" – from the take-off to 168th interval of time recorded on the recorder tape; stage "B" from 68 to 174,2 and stage "C" from 174,2 to the crash. The analysis of records makes possible the claim that the flight until 168th time marker on the tape goes smoothly. Starting with 168th interval of time a diverging from the norm character of deflection of the tail plane occurs and changes of vertical G-load caused by it.
As a result of analysis of the record it was determined, that the work of the automatic pilot was without reservations until the 168th time marker on the tape. At that moment of flight of the aeroplane, one can observe a diverging from the norm character of deflection of the tail plane and, as an effect, changes of vertical G-load. Changes of G-load with quite significant amplitudes point to their relationship with the change of attack angle and aeroplane pitching angle. At that time the automatic pilot was working, probably in the "Stabilization" range (system SARPP-12 does not distinguish the ranges of work of the automatic pilot).

The considerations of possible causes of formation of such vibrations were divided into three groups:

1. Vibrations caused by atmosphere turbulence with correct operation of AP-155SN.
This cause can be discarded with high probability for two reasons:
– meteorological conditions according to assessment made by specialists did not point at the possibility of turbulence occurring;
– vibrations did not occur after switching off the automatic pilot.
2. Vibrations caused by excitation of the hydraulic amplifier with correct operation of the automatic pilot.
This cause can also be discarded with high probability because of the fact that after switching the automatic pilot off until the end of the flight faulty operation of the amplifier is not observed.
3. Vibrations caused by unserviceability of the AP-155SN automatic pilot.
This is the most probable cause of the occurrence of vibrations. Because of the fact that it is impossible to recreate the operation of the automatic pilot, the considerations concerning the possible unserviceabilities causing vibrations of this type are hypothetical.
There are many reasons which may cause such vibrations. These include:
a.) Lack of appropriate transpositions in the automatic pilot.

Because of correct operation of the automatic pilot for most of the flight incorrect ground service of technical personnel should be ruled out. Maladjustment of transpositions during aeroplane flight is theoretically possible, though improbable.
b.) Damage of corrector of spectral system of automatic transposition shift in the vibration damping loop of the automatic pilot.

This is a part of the adaptation system, the main task of which is automatic shift of transposition in relation to angular velocity of pitching in the perimeter of damping of aeroplane short-term vibrations.

Damage is quite probable.
c.) Damage or stoppage in electric circuit of DOS.

It is a system, the task of which is the measurement of current deflection of the tail plane for the needs of analysis of signal in spectral corrector of adaptation system.

This damage is also quite probable.

d.) Damage of electric servo-propulsion.

It is a system consisting of two blocks: BUM-2M and RAU-107A. From among the possible kinds of damages in this case the ones that can be taken into consideration are: maladjustment of phase dislocation, which influences the change of servo-propulsion dynamics, and in effect the possibility of occurrence of aeroplane vibrations.

Damage theoretically possible.

e.) Damage in follow-up system of forming of the given value of pitching angle.

This system consists of commutation perimeters, among others: micro switches on the control stick, selsyn system, amplifier and electric engine with transmission. The effect of this type of damage would be visible with simultaneous influence of operator-pilot on the control stick and of the automatic pilot. The influence of the automatic pilot could interfere, in this case, with the influence of the operator-pilot. This damage is also quite probable.

Many probable reasons of the faulty operation of the automatic pilot causing such aeroplane reaction can be mentioned. Only the ones which on the basis of self-made experiments and analysis of technical documentation seem the most probable are presented in this study.

Summing up the assessment of operation of the automatic pilot, one can claim that one of the most probable causes can be the damage of micro switches on the control stick working together with the follow-up system of forming the given value of pitching angle. Signal to deflect the tail plane in the considered time period has, apart from oscillatory, also stochastic or deterministic character, caused probably by the influence of operator-pilot. This signal recorded by the SARPP-12 system is a resultant signal: of the action of operator-pilot, automatic pilot and trimmer effect mechanism. The influence of the operator-pilot on the control stick in the considered time period could be the effect of not only intended control process but also counteraction to faulty signals made by the automatic pilot, which occurred as a result of damage.

Nevertheless, it seems that damage of the automatic pilot should not have a direct relationship with the air crash that occurred. The pilot switched off the automatic pilot. The vibrations of the aeroplane subsided. At that moment the aeroplane had a significant reserve of altitude (more than 3000 m with the velocity of around 500 km/h) and full control of manual control of the aeroplane.

Because of the fact that SARPP-12 recorder recorded only parameters of aeroplane longitudinal flight, full and unambiguous reconstruction of the flight is practically impossible. It is possible to rule out certain flight trajectories, yet there will always remain an ensemble of various trajectories, which can be termed probable. From the mathematical point of view aeroplane flight is described with six ordinary differential equations of second order, which should be supplemented with six differential equations of kinematic relationships. This means, that for unambiguous determination of flight parameters, 12 parameters determining initial flight parameters and control laws are needed. The record of the recorder provides information about six (longitudinal) flight parameters. Therefore the recreation of flight with the method of computer simulation requires assuming a flight scenario allowing for determination of initial flight parameters and assuming the control of ailerons and the rudder. With the use of the method of elimination of solutions (in this case analysis of coefficient of G-load and flight trajectory) one can rule out the results of simulation which do not provide a course of changes in time of $n_z=f(t)$ (G-load coefficient) and $H=g(t)$ (flight altitude) similar to the one recorded in-flight.

Analysis of the record of SARPP recorder inclines one to assume the following scenario of the final two stages of the investigated flight. At the moment corresponding with 168^{th} interval of the record on the recorder tape an abnormal record of deflections of the stabilizer appears and oscillations of the G-load coefficient following it. The most probable reason of this phenomenon was a malfunction of the automatic pilot. The analysis of the possible and most probable causes of that malfunction was given above. The record of SARPP-12 recorder

(fig. 4.80) can be a proof of problems arising in correct control of the aeroplane. In 169th interval of the record $n_z=f(t)$ of the recorder and increase of value n_z ($n_z \cong 3$) occurs, which can be interpreted as the entering of the aeroplane into another turn. In flight simulation it was assumed, that it is a left turn changing the course of the aeroplane from 360 to approximately 240 degrees. A moment after entering the turn, the problems of the pilot with maintaining flight parameters occur (a significant change of velocity, flight altitude and G-load coefficient). Characteristic oscillations of the record of angle of deflection of the stabilizer and of the G-load coefficient also occur. It looks as if the pilot was "fighting" with the aeroplane. This may signify that the damaged automatic pilot was significantly interrupting correct controlling of the aeroplane. After around 20 s (time marker 171) it was assumed, that the aeroplane was leaving the turn and starting to decrease altitude.

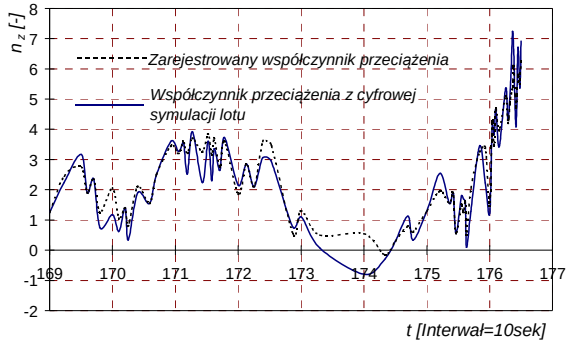

Fig. 13 Simulation of MiGa-21 bis crash. Course of *g*-load coefficient n_z.

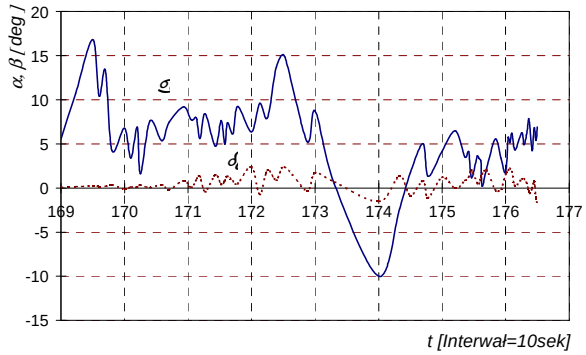

Fig. 14 Simulation of MiGa-21 bis cash. Course of angles of attack α and slip β

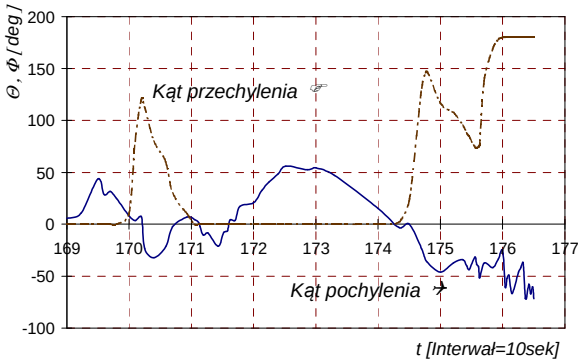

Fig. 15 Courses of angles of pitch and bank

The following approximately 40 seconds of flight was interpreted as a pull-up from level flight. In the peak position of the aeroplane, corresponding with 174.2 time marker on the tape of the recorder, a switching off of the automatic pilot was recorded. With the help of flight simulation, for time corresponding with value 174.2 of the marker flight velocity of the order of 115 m/s was obtained, pitching angle of the aeroplane was around -20º, banking angle of the order of 0º, attack angle around -5º, g-load coefficient n_z= -0.2. A moment later the aeroplane banks left, after 10 s getting the banking of the order of -100º, the pitching angle is around -40º. In 175 interval of time the aeroplane goes into clouds. In the clouds a loss of spatial orientation must have happened, as a result of which the aeroplane in 176 interval of time hit the sea surface. Pitching angle of the aeroplane at the moment of the hit, obtained with the use of simulation was around -60º, banking angle of the order of -100º, and aircraft yawing angle 70º.

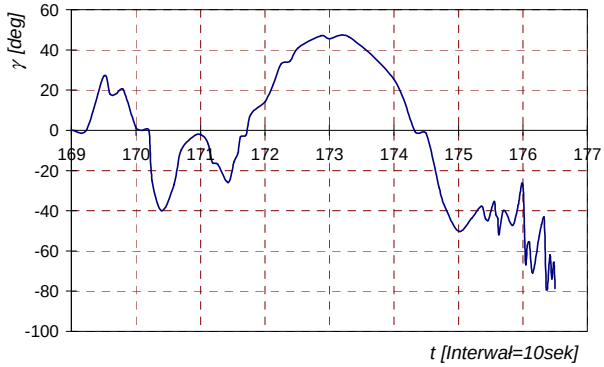

Figure 16 Course of flight path angle

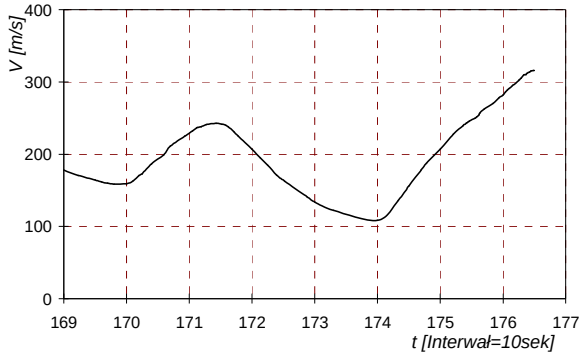

Figure 17Course of airspeed *V*

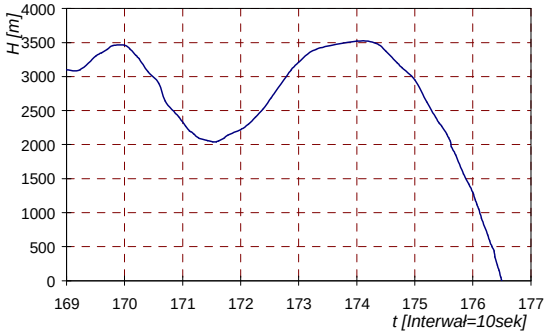

Figure 18 Course of flight altitude *H*.

On the basis of the assumed scenario, confirmed by correct results of the computer simulation it can be stated, that the accident occurred because of a series of unfavourable circumstances and pilot mistakes. The direct cause of the crash was a loss of spatial orientation by the pilot when going through clouds. An indirect cause was a malfunction of the automatic pilot, which caused a discomfort of pilot's operation. Switching the automatic pilot off at the peak point of a pull-up from level flight in conditions of unsteady flight on a relatively low flight velocity and relatively large negative attack angle could have caused a stall of the aeroplane in the direction of a wing. Ceasing of aeroplane vibrations could have caused the pilot to relax for a moment. This can explain the fact, that for around 10 seconds the aeroplane was reducing its altitude with quite high pitching angle and banking angle in relation to the clouds. Undoubtedly the pilot did not consider the flight in that time span dangerous. Otherwise he would have undoubtedly corrected the flight.

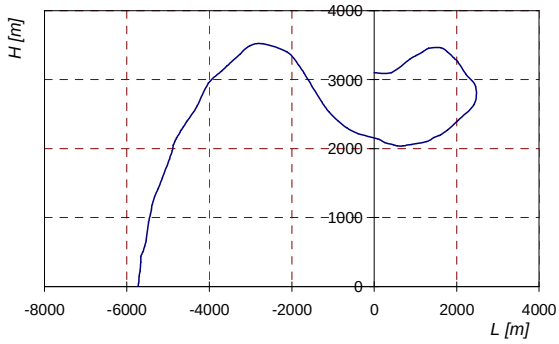

Fig. 19 Simulation of MiGa-21 bis crash. Flight trajectory.

The lack of appropriate action since entering the clouds caused a dangerous situation while flying within the clouds. As a result of a loss of spatial orientation during going through the clouds an incorrect action was undertaken by the pilot which led to the crash. Because of the permissible values of normal G-\coefficient it can be assumed, that a safe pull-up from the dive was possible at flight altitude no less that 150m. This means, that after coming out of the clouds (because their basis was smaller that 550m), a pull-up of the aeroplane from the dive was impossible. The results of computations are presented in figures 11 – 17.

6.4. Fatal accident of TS-11 Iskra yet trainer caused by icing [59]

Icing consists in a thick ice coating developing on the surface of the aeroplane. It creates a significant danger and threat in flight. Deformation of profiles of lifting surfaces of the aeroplane by the ice occurs: the wings, tail plane, vertical tail unit, control surfaces, icing of: the cockpit, air intakes into the engines, air pressure receiver (APR), etc. Icing causes: rapid decrease of maximal value of aerodynamic lift coefficient C_{Zmax}, decrease of critical attack angle α_{kr}, increase of aeroplane mass and increase of aerodynamic drag.

Lately nine crashes of communication aeroplanes caused by icing were recorded. In these crashes 286 people died. The crashes of the following aeroplanes can be mentioned here: ATR 42 (1987 Italy), F 28 (1989 Canada), MD 80 (1981 Sweden), F 28 (1992 USA), Fokker 100 (1993 Macedonia), ATR 72 (1994 USA), 19AN 24 (1995 Italy). To the mentioned communication crashes also icing-caused

crashes of touristic, sport, military aeroplanes and other aircrafts (e.g. helicopters) need to be added. One should also mention crashes of Polish aircrafts caused by icing, e.g. An-24 no. 12 aeroplane near Szczecin (28. 02. 1973), TS-11 „Iskra" no 1H0713 military aeroplane near Otwock (11. 11. 1998), Mi-2 no 3047 military helicopter (5. 11. 1981), Mi-8T no 19-0615 helicopter (01. 12. 1983), Su-22M4 no 37714 aeroplane (30. 01. 1990), or the recent malfunction of Mi-8 no 632 helicopter (04. 12. 2003).

First researches on icing were conducted even before 2nd World War. One could mention here the pioneer research made in 1938 by Göttingen Institute of Aerodynamics [82]. This happened shortly after recording first crashes caused by icing in the thirties (e.g. such accident happened in Switzerland, where because of icing DC-2 aeroplane had crashed). During tunnel research in Göttingen in 1938 "rime" type icing was obtained on the wing profile and clear ice on the wing nose – fig. 32 [82].

After the war this research was and still is intensively conducted in many science centres, e.g. NASA and research facilities of aircraft companies e.g. Martin Lockheed, Fokker, Boeing, Aerospatiale, British Aerospace [12, 13, 17, 59, 71, 75, 95]. Lately research of icing of the aeroplane has also been undertaken in Poland. One could mention here research of icing of elements of the aeroplane and segments of the wing, conducted at the Institute of Aviation Technology at the Mechatronics Faculty of Military Technical Academy (WAT) and at the Faculty of Aerodynamics of Institute of Aeronautics and Applied Mechanics of the Warsaw University of Technology. [59].

The phenomenon of icing occurring in the atmosphere is one of the more difficult problems of aviation meteorology. It is difficult to forecast and moreover, it repeatedly occurs in identical meteorological conditions with various intensity, often with the speed of build-up of the ice layer over 2 mm/min. The most frequent and most dangerous kinds of icing occur in the temperature range from –5°C to 0°C [12, 13].

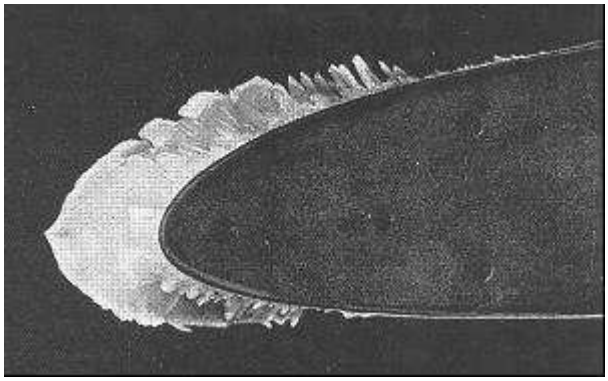

Figure 27 "Rime" type icing on the wing profile got in a wind tunnel (Göttingen 1938 [120])

The main reason of icing is the freezing of over-cooled drops of water, which after hitting the airframe freeze creating an ice layer [1, 14, 18, 90, 118, 168]. The intensity of icing is directly proportional to the amount of water in the air (LWC – *liquid water coefficient* [g/m^3]) and the dimensions of water drops (MVD – *median volumetric diameter* [μm]).

0The lower the temperature the smaller the water drops. Small drops with diameter below 0.5 mm freeze directly after hitting the airframe, are crystallized fast causing the formation of marble ice [12]. Because of the form of icing, the most dangerous is icing with clear ice. It is formed in temperature from -10°C to 0°C and with large diameters of drops, the ice layer can be formed deep within the aerofoil. With stratocumulus, stratus and nimbostratus clouds and temperatures from –5°C to 0°C there is a possibility of intensive icing.

6.4.1. Influence of icing on aerodynamic characteristics of an aeroplane

Aircraft icing is manifesting by:

- icing of lifting surfaces: wings, tail plane, vertical tail unit,
- increase of aeroplane mass m,
- decrease of aerodynamic lift coefficient C_{Zmax},
- increase of drag force coefficient C_X ,
- decrease of critical attack angle α_{kr},
- shift of centre of mass of iced aeroplane forward – aeroplane "heavy on the nose",
- icing of air intakes to engines,
- icing of the cockpit,
- icing of Pitot tube (OCP),

– incorrect indications or no indications of: device velocity V_p (velocity meter), barometric altitude H_p (altimeter), velocity of climb (rate-of-climb indicator) Mach number (Machmeter).

Tunnel tests of Fokker F-28 aeroplane with a wing with "abrasive paper" type fouling showed 25% reduction of maximal aerodynamic lift and 6° reduction of critical attack angle [13]. McDonnell-Douglas company notes, that the fouling of the surface only 0.4 mm thick on the wings of DC-9-10 aeroplane can be the cause of loss of 25% of aerodynamic lift and loss of critical angle to the value below that, which switches on the warning system (of transgression of α_{kr}). This was confirmed by research done by Boeing, as well as tunnel research and simulation computations by NASA [13, 17]. One needs to remember, that icing develops strongly on the edges of attack of lifting surfaces [17], which creates the greatest danger especially for aeroplanes having profiles of lifting surfaces of little relative thickness. (fig. 34 [13]) – profiles sensitive to separation. Especially aeroplanes which have no anti-icing system of the airframe become defenceless and in many cases the pilot is unable to prevent the crash

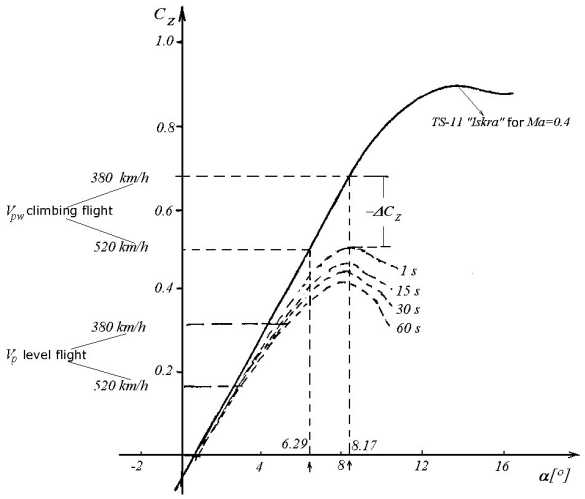

Fig.ure 28 Influence on icing on coefficient of aerodynamic lift of the aeroplane: assumed for TS-11 "Iskra" aeroplane changes $C_Z(\alpha)$ (on the basis of T. Cebeci 1996 [17]).

6.4.2. A study of influence of icing on the dynamics of aeroplane climbing flight

The most dangerous phase of flight is going from level flight to climbing within clouds with icing present. The aeroplane decreases device velocity which causes a decrease of aerodynamic lift proportional to squared velocity. When going to higher attack angles while climbing the aeroplane can enter the range of strong decrease of aerodynamic lift coefficient caused by icing – figure 28. The decrease of flight velocity V_p and the decrease of C_{Zmax} can cause the aeroplane to enter supercritical attack angles $\alpha > \alpha_{kr}$ (fig.ure 29) and, as a result of a shortage of aerodynamic lift with full engine thrust, it can lead to dynamic stall.

The most dangerous for an aeroplane that is being iced is not the increase of mass ΔG (figure 30), but the changes of aerodynamic characteristics occurring in a very short time during the first seconds of icing fig. rys.34 [55].

$$\Delta P_{Za}^{l} = \frac{1}{2}\rho S\left(V_p^2 - V_{pw}^2\right)\cdot C_Z^{l}(\alpha) \qquad (13)$$

where:

V_{pw} – device velocity while climbing

$V_{pw} < V_p$;

$C_Z^{l}(\alpha) < C_Z(\alpha)$; $\alpha_{kr}^{l} < \alpha_{kr}$

$C_z^{l}(\alpha)$ - aerodynamic lift coefficient of an aeroplane which is being iced

As it has already been mentioned, the icing of an aeroplane causes not only an increase of aeroplane mass, but is also the cause of degradation of aerodynamic characteristics. This is made explicit mostly by a decrease of the aerodynamic lift coefficient of the aeroplane, a decrease of the value of critical attack angle and an increase of drag coefficient of the aeroplane [13].

Research done by professor Tuncer Cebeci of California State University prove, that even a very slight icing of a lifting surface can cause radical decrease of critical attack angle, to quote [13]: „(...) *Event 1st ice is sufficient to cause a drastic change in the stall angle* (...)". The process of degradation of aerodynamic lift coefficient and decrease of critical attack angle is presented in figure 3. This figure illustrates the change of character of changes of aerodynamic lift coefficient in function of attack angle after time 1, 5, 15, 30 and 60 seconds since the moment of beginning of icing. These

results were obtained with static temperature of flow 260,44°K, static pressure p=90754 Pa, liquid water content of cloud LWC=0,50 g/m^2, stream velocity V =129 m/s, and diameter of drops 20μm.

Analysis of fig. 4.97 shows, that in the range of small attack angle (up to 5 degrees) the influence of icing on lifting characteristics of the profile is little and can go unnoticed by the pilot. A very important matter is the drastic decrease of critical attack angle (reaching 50% even after the first second of icing). Therefore the initial phase of icing is particularly dangerous in case of flight with higher attack angles. This is because involuntary stall of the aeroplane can occur. It needs to be emphasised, that the cause of the decrease of critical attack angle in the first phase of icing are the phenomena occurring in the boundary layer (the model concerns the layer of ice on the edge of attack of thickness not larger than 1 mm). The experimental data presented above was verified with the use of computations done by *LEWICE* programme (compare [13]).

On the basis of the model of the aeroplane presented in the first chapter and the model described by Cebeci a simulation of climbing flight of an aeroplane in conditions of icing of lifting surfaces was performed. It was assumed, that the effect of changes ΔC_z in time function can be obtained with the use of relationship:

$$\Delta C_z = \Delta C_{Z\infty}\left(1-e^{\lambda t}\right) \qquad (14)$$

The computations were made for several values of λ coefficient (from formula 25). The change of course of function $C_Z(\alpha)$ (from linear to non-linear) causes a change of pitching moment (change of position of centre of pressure of the aeroplane). This change was estimated from relationship:

$$\Delta x_p = x_p\left(\frac{1}{1-\Delta C_z/C_z}-1\right) = x_p k_{x_p} \qquad (15)$$

Results of computations are presented in figures 30 - 38.

Figure 37, presenting the course of G-load coefficient in time function, is especially interesting. The value of n_z, practically to the moment of aeroplane stall has a value close to one. Such course of n_z can give evidence to the fact, that the crew of the aeroplane during the entire flight may not be aware of the gravity of the situation. Figures 34, 38 present the course of angles of pitching and of banking of the aeroplane. In the case when the process of degradation of aerodynamic lift of the aeroplane rises slowly (λ=-0.1) in the assumed time the aeroplane does not hit the ground. The values of angular velocities, the exemplary course of which is presented in fig. 30 are little (of the order of 1°/s). Figure 38 presents trajectory of aeroplane flight.

The model of icing of the aeroplane presented above leads, as an effect, to the occurrence of very dangerous situation during flight, especially in conditions of going to larger attack angles (e.g. after going from level flight to climbing flight). Because of the fact, that the process of degradation of flying qualities of the aeroplane goes violently, not giving any "warning marks" noticeable by the pilot, such as e.g. occurrence of vibrations of the aeroplane, or change of balancing conditions (mass of increasing ice is low in this phase of icing), this phenomena can be recognised as extremely dangerous. The courses of flight parameters obtained by digital simulation show, that the assumed model of icing can as a consequence lead to aeroplane crash.

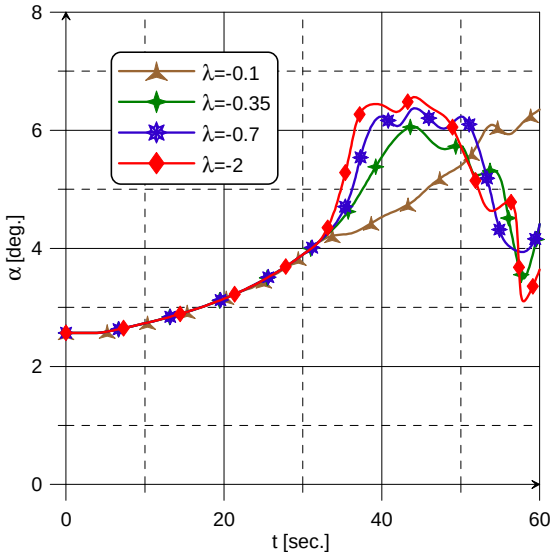

Figure 30 Simulation of icing – course of $\alpha(t)$

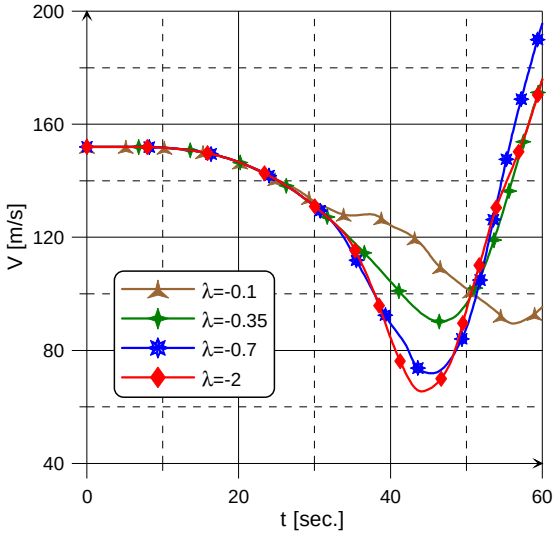

Figure 31 Simulation of icing – course of $V(t)$

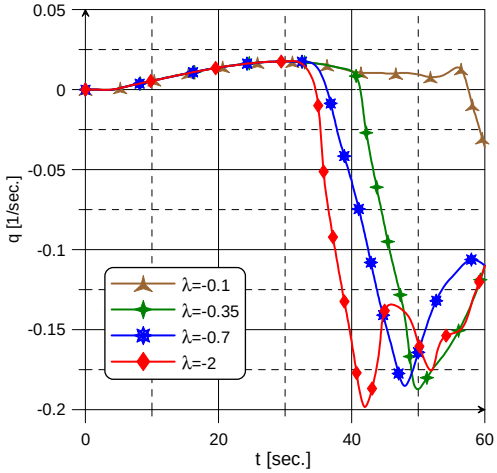

Figure 32 Simulation of icing – course of $Q(t)$

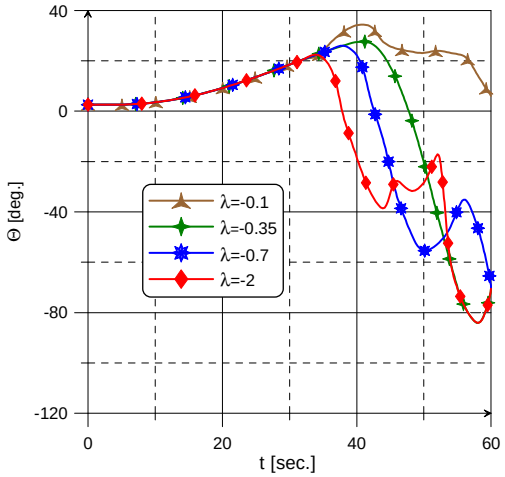

Figure 33 Simulation of icing – course of $\Theta(t)$

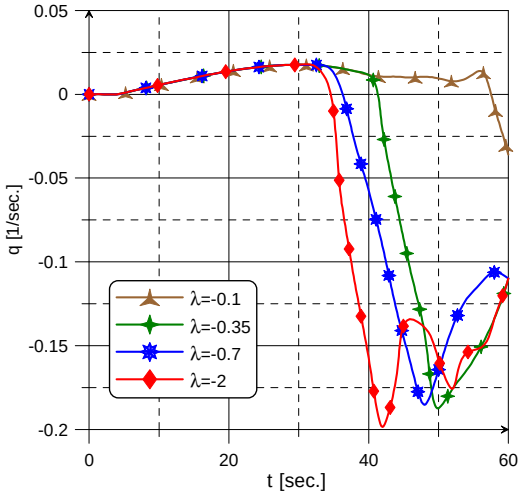

Figure 34 Simulation of icing – course of $Q(t)$

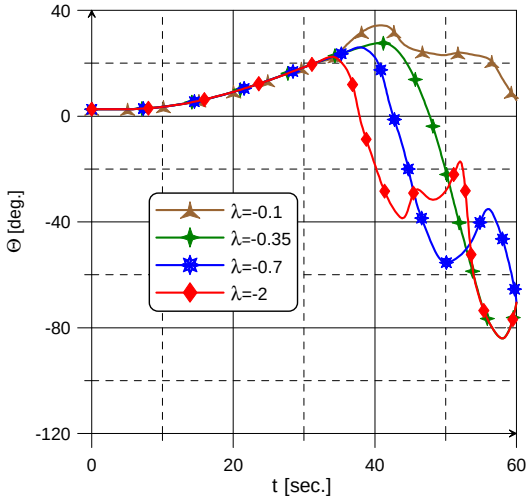

Figure 35 Simulation of icing – course of $\Theta(t)$

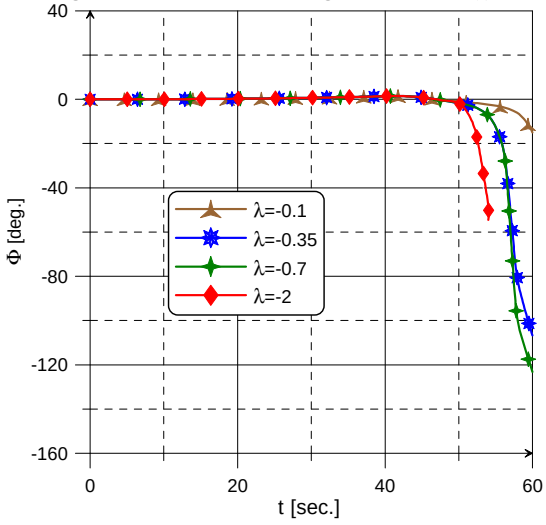

Fig.ure 36 Simulation of icing – course of $\Phi(t)$

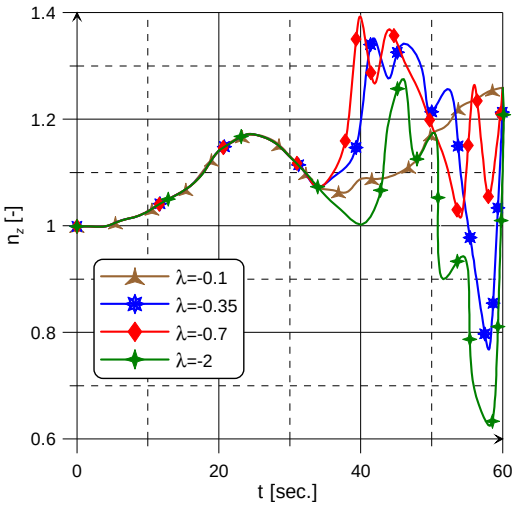

Figure 37 Simulation of icing – course of $n_z(t)$

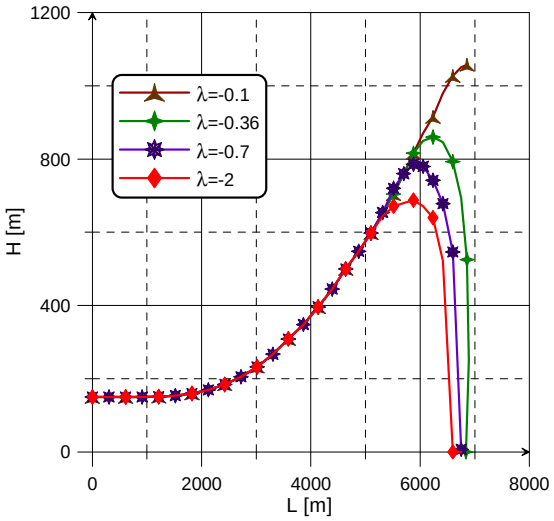

Figure 38 Simulation of icing –flight trajectory

6.4.3. The cause of the TS-11 "Iskra" yet trainer crash (near Otwock, 11th November 1998)

Lack of records of flight parameters creates an especially difficult task for the people investigating an air crash. Then, sometimes the only information are the records of conversations made by the crew, pictures of the scene and sketches of it, possible accounts of witnesses and of course thorough analysis of the wreckage. Many times in such case it is necessary to assume hypothesis of causes of the occurrence.

A classic case of such occurrence is the *casus* of crash of TS 11 "Iskra" training aeroplane no1H0713, which happened on November the 11th 1998 near Otwock. This aeroplane was one of the crafts of "Sparks (Iskry) Acrobatic Team" (presently "Red-and-White Sparks". Because of the specificity of aerobatic crafts the so-called "black box" was not installed on it, therefore there were practically no records of flight parameters. The only recorded parameter was the profile of flight recorded by the radar of a ground flight control station. On the basis of that record the course of changes of flight velocity was recreated, practically up to the moment of collision with the ground (presented in fig. 39).

Below an attempt of reconstructing this crash will be presented, basing on the hypothesis, that the direct cause of that tragic occurrence was icing of lifting surfaces. The crash took place near Otwock, while performing weather test flight before a planned flight of the team over the Piłsudskiego Square in Warsaw on Independence Day.

Right before the crash "Iskra" was flying with cruising velocity V≈ 520 km/h at altitude 100-200 m all the time being below the basis of clouds (*stratus* type clouds) with the danger of icing present. Because of weather conditions getting worse continuously (the basis of the clouds lowering to 0 level) and the danger of hitting an obstacle connected with that the pilots decided to climb above the clouds level. They reported their intention to ground flight control and got approval of such a manoeuvre.

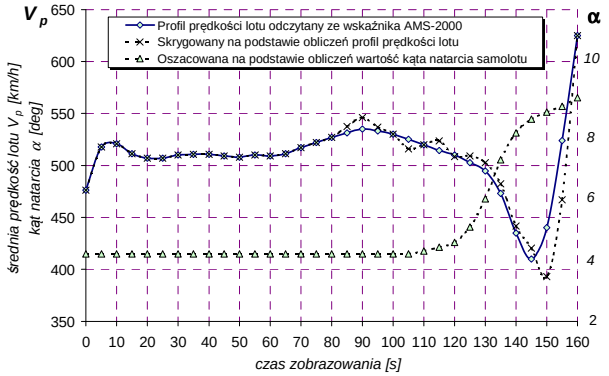

Figure 39 Profile of flight velocity *Vp* from *AMS-2000* indicator (on the basis of [173]) with drawn, in accordance with computations change of attack angle α and proper correction of flight profile [59]

According to weather conditions observed that day the temperature within the clouds was falling to approximately -5°C. Meteorological

data also showed on the presence of the phenomenon of inversion within the clouds, which in turn favoured liquid water content of the cloud. Over-cooled water drops falling on coating could cause intensive icing of the aeroplane. Ice building up on the wing profile caused a slight (disregardable) increase of aeroplane mass, yet, in accordance with the data of many studies made among others by Cebeci [18], Bragg and others [13], significant (reaching 50%) decrease of aerodynamic lift coefficient C_z and around 45% decrease of critical attack angle α_{kr}. Decrease of aerodynamic lift (ΔP_z) is caused both by decrease of velocity (V_p^2 in a square) and by the decrease of aerodynamic lift coefficient $\Delta C_z = C_z - C_z^l$.

Among the causes of TS-11 "Iskra" aeroplane crash (November the 11th 1998, near Otwock), the most serious hypotheses of its cause were:

- loss of spatial orientation while going through the clouds;
- dynamic stall caused by icing of wings during climbing flight inside the clouds.

More interesting case for cognitive purposes is the dynamic stall caused by icing of lifting surfaces. The results of simulation of climbing flight in conditions of intensive icing are presented in fig. 40 ÷fig. 45. When analysing these diagrams one can claim, that the hypothesis stating that the direct cause of the crash was icing is probable. Because of a rapid decrease of aerodynamic lift and increase of aerodynamic drag dynamic stall of the aeroplane occurred. Pitching, the aeroplane went into uncontrollable dive with simultaneous yawing right and banking towards the right wing, caused by gyroscope effect of left-turning turbine reaction engine. Because of time shortage since the moment of stall to hitting the ground the crew was unable to react.

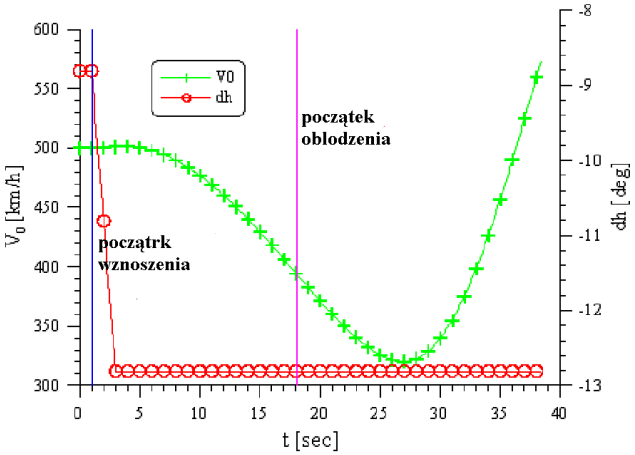

Figure 40 Reconstruction of TS-11 "Iskra" aeroplane crash. Course of flight velocity and change of the angle of deflection of the elevator.

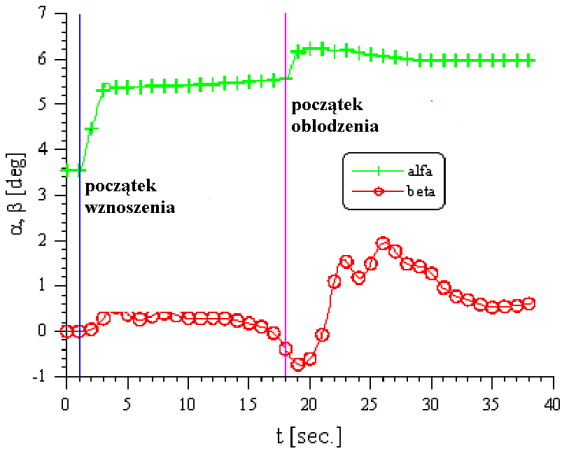

Figure 41 Reconstruction of TS-11 "Iskra" aeroplane crash.. Courses of angles: of attack and of slip.

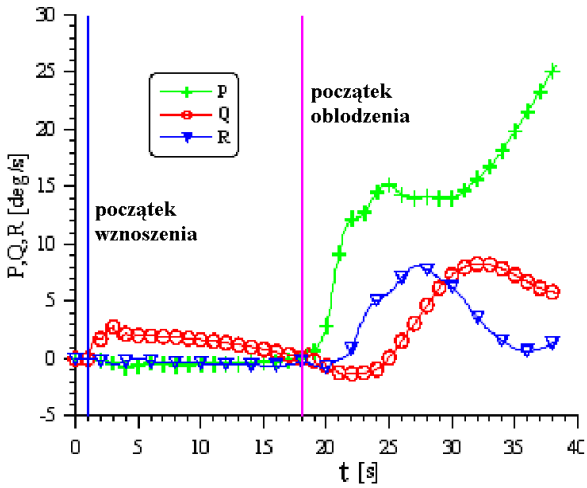

Figure 42 Reconstruction of TS-11 "Iskra" aeroplane crash.. Courses of angular velocities of: pitching *Q*, banking *P* and yawing

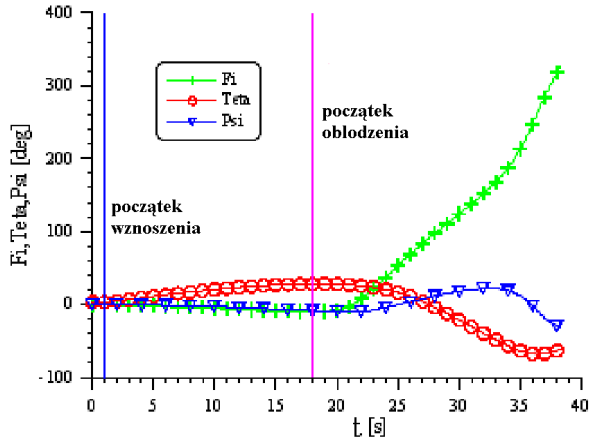

Figure 43 Reconstruction of TS-11 "Iskra" aeroplane crash.. Courses of angles of: pitching banking and yawing

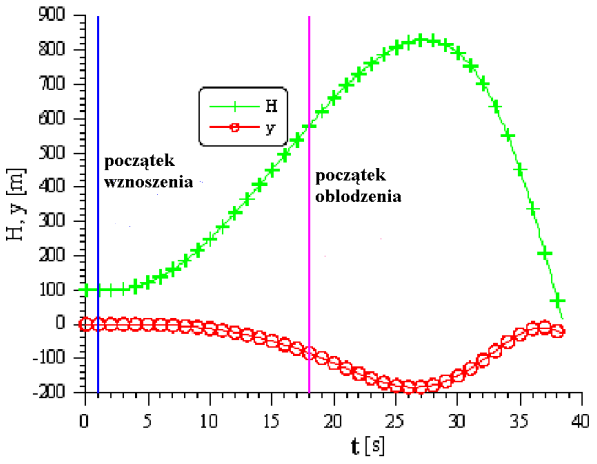

Figure 44 Reconstruction of TS-11 "Iskra" aeroplane crash.. Course of aeroplane flight path.

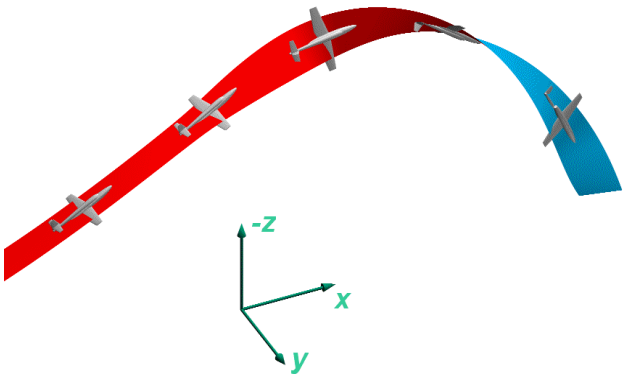

Figure 45 Reconstruction of TS-11 "Iskra" aeroplane crash. Trajectory of flight (three-dimensional view)

It should be noted, that in the remarks on winter operation for communication pilots [94], the regulations end in words: "(...) *Do not belittle icing. Change of aerodynamic properties of the aeroplane in real strong icing is difficult or even impossible to predict by the constructors and test pilots during test flights.* (...) *The anti-icing system should only help you to safely leave icing zone – it does not guarantee a safe flight in such conditions!*".

Conclusions

In this paper we give into LOC based on the control analysis of the flight dynamics. We show how the controllability properties of the aircraft diminish near critical points of the trim equations, (for example stall). Our results show that when operating near stall control properties can change fundamentally with small changes in the aircraft state. Thus a small disturbance can cause a dramatic change in how aircraft responds to pilot inputs. The method can be easily applied to systems in non-normal situations, especially those that can be modeled with parameter variation, such as aft center of mass or icing.

The anatomy of disasters and accidents in complex technological systems, such as the latent failure model of complex systems, such as aviation, show an aetiology that is reflected in the latent failure model of complex system. Building on the foundation of human error as proposed by Reason, a model is described that helps explain the nature of aviation accidents. Situational factors and systemic factors (latent conditions) are mapped onto the cusp catastrophe model in facilitate a descriptive and predictive illustration of the dynamics of situational factors and latent conditions to help explain the nature of aviation accidents. The model, by way of its failures, illustrates the trigger effect of active features, illustrates the trigger effect of active failures (captured within the situational factors) and how it precipitates the systemic conditions, resulting in a disastrous outcome. We used four tragic aircraft crash as example of how the control factors of the cusp catastrophe combine to create a situation whereby instability ensues and a catastrophic event occurs.

Contact Author Email Address

krzysztof.sibilski@pwr.wroc.pl
sibilski@hot.pl

References

[1] AGARD Adv Rpt 314, Operational agility Apr 1994.

[2] AGARD Advisory Report No. 155A. Manoeuvre Limitations of Combat Aircraft,

[3] AGARD Advisory Report No. 265, Rotary-Balance Testing for Aircraft Dynamics, 1990.

[4] Avanzini G., De Matteis G., Bifurcation Analysis of a Highly Augmented Aircraft Model, *Journal of Guidance, Control & Dynamics 1998, Vol.20, No.1.*

[5] Bajpai G., Beytin A., Thomas S., Yasar, M., Kwatny, H. G., Chang, B. C., "Nonlinear Modeling and Analysis Software for Control Upset Prevention and Recovery of Aircraft" *AIAA Guidance, Navigation and Control Conference*, AIAA, Honolulu, Hawaii, 18-21 August 2008.

[6] Berg J., Kwatny H. G., "An Upper Bound on the Structurally Stable Regulation of a Parameterized Family of Nonlinear Control Systems" *Systems and Control Letters* , Vol. 23, 1994, pp. 85–95.

[7] Berg, J. M., Kwatny, H. G., "Unfolding the Zero Structure of a Linear Control System, *"Linear Algebra and its Applications* , Vol. 235, 1997, pp. 19–39.

[8] Bitsoris, G. and Gravalou, E., "Comparison Principle, Positive Invariance and constrained regulation of Nonlinear Systems," *Automatica* , Vol. 31, No. 2, 1995, pp. 217–222

[9] Bitsoris, G. and Vassilaki, M., "Constrained Regulation of Linear Systems," *Automatica* , Vol. 31, No. 2, 1995, pp. 223–227227.

[10] Biushgens, G. S. and Studnev, R. V. *Aircraft Dynamics. Spatial Motion*, Mashinostorenie, Moscow, 1983,, Publishers (in Russian).

[11] Blanchini, F., "Feedback Control for Linear Time-Invariant Systems with State and Control Bounds in the Presence of Uncertainty," *IEEE Transactions on Automatic Control* , Vol. 35, No. 11, 1990, pp. 1231 – 1234.

[12] Bradburg F.: *Meteorology and flight – apit'os quite to weather*, A&C Black, London 1996.

[13] Bragg M. B., et all.: Effect of ice accretion on aircraft flight dynamics, *AIAA-2000-0360CP*, Reno, January, 2000..

[14] Brandon J., M.: Dynamic stall effects and application to high performance aircraft. Spetial course on aircraft dynamics af high angles of attack: experiment and modeling, *AGARD Report No. 778*, April, 1991.

[15] Calkins D. E.: Aircraft accident flight patch simulation and animation, *Journal of Aircraft*, Vol. 31, No 2, 1994.

[16] Carroll J. V., Mehra R. K., Bifurcation Analysis of Non-Linear Aircraft Dynamics, *Journal of Guidance Control and Dynamics*, Vol. 5, No. 5, 1982. pp. 529-536.

[17] Cebeci T.: Effect of ice on airfoil stall at high reynolds numbers, *AIAA Journal*, vol. 33, no. 7, 1995.

[18] Chapman G. T., Tobak M., Nonlinear problems in flight dynamics, NASA-TM-85940, May, 1984.

[19] Charles G. A., et. all., Aircraft Flight Dynamics Analysis and Controller Design Using Bifurcation Tailoring, *AIAA Guidance, Navigation and Control Conference Technical Papers*, USA, 2002, AIAA-2002-4751-CP, American Institute of Aeronautics and Astronautics.

[20] Charles, G. A., Lowenberg, M. H., Wang, X. F., Stoten, D. P., and Bernardo, M. D., "Feedback Stabilised Bifurcation Tailoring Applied to Aircraft Models," *International Council of the Aeronautical Sciences 2002 Congress* , 2002, pp. 531.1– 531.11.

[21] Croom, M., Kenney, H., Murri, D., Lawson, K., "Research on the F/A-18E/F Using a 22Flight Mechanics Confer- ence", Denver, 2000.

[22] Dam, ten A. A. and Nieuwenhuis, J. W., "A Linear programming Algorithm for Invariant Polyhedral Sets of Discrete- Time Linear Systems," *Systems and control Letters* , Vol. 25, 1995, pp. 337–341.

[23] Dietenberger M. A., Haines P. A., Luers J. K.: Reconstruction of Pan Am New Orleans accident, *Journal of Aircraft*, Vol. 22, 8, 1985.

[24] Ermentrout B., *Simulating, Analyzing, and Animating Dynamical Systems. A Guide to XPPAUT for Researchers and Students*, SIAM, Philadelphia, 2002.

[25] Etkin B.: *Dynamics of Atmospheric flight*, Ed. John Willey, N. York, 1972.

[26] Feuer, A. and Heymann, M., "Ω-Invariance in Control Systems wiyh Bounded Controls," *Journal of mathematical Analysis and Applications* , Vol. 53, 1976, pp. 26–276.

[27] Foster, J. V., Cunningham, K., Fremaux, C. M., Shah, G. H., Stewart, E. C., Rivers, R. A., Wilborn, J. E., and Gato,W., "Dynamics Modeling and Simulation of Large Transport Aircraft in Upset Conditions," *AIAA Guidance, Navigation, and Control Conference and Exhibit* , San Francisco, CA, 15-18 August 2005.

[28] Glover, J. D. and Schweppe, F. C., "Control of Linear Systems with Set Constrained Disturbances," *IEEE Transactions on Automatic Control* , Vol. 16, No. 5, 1971, pp. 411–423.

[29] Goman M.G., Khramtsovsky A.V., Application of continuation and bifurcation methods to the design of control systems. *Phil. Trans. R. Soc.*, No. A 356, London, 1998, pp 2277-2295.

[30] Goman, M. G., Zagainov, G. I., and Khramtsovsky, A. V., "Application of Bifurcation Methods to Nonlinear Flight Dynamics Problems," *Progress in Aerospace Science* , Vol. 33, 1997, pp. 539–586.

[31] Goman, M. and Khrabrov, A., State-space representation of aerodynamic characteristics of an

aircraft at high angles of attack, *J. Aircraft* , vol.31, no 5, 1994, pp. 1109-1115.
[32] Guckenheimer J., Holmes J., *Nonlinear Oscillations, Dynamical Systems, and Bifurcations of Vector Fields*, Springer, N. Y., 1983.
[33] Guicheteau P., Bifurcation theory applied to the study of control losses on combat aircraft, *La Recherche Aerospatiale*, no. 2, 1982, pp. 61-73.
[34] Guicheteau P., Bifurcation Theory: a Tool for Nonlinear Flight Dynamics, *Phil. Trans. R. Soc.*, No. A 356, London, 1998, pp 2181-2201.
[35] Guicheteau, P. Stability analysis through bifurcation theory (1 and 2); and nonlinear flight dynamics, in Nonlinear Dynamics and Chaos, AGARD Lecture Series 191, June 1993.
[36] Guicheteau, P., Bifurcation theory in flight dynamics. An application to a real combat aircraft, ICAS Paper 90-5.10.4, September 1990.
[37] Holleman, E. C., "Summary of Flight Tests to Determine the Spin and Controllability Characteristics of a Remotely Piloted, Large-Scale (3/8) Fighter Airplane Model," Tech. Rep. NASA TN D-8052, NASA Flight Research Center, January, 1976 1976.
[38] Hossain, K. N., Sharma, V., Bragg, M. B., Voulgaris, P. G., "Envelope Protection and Control Adaptation in Icing Encounters," *41st AIAA Aerospace Sciences Meeting and Exhibit* , Reno, Nevada, 6-9 January 2003.
[39] Hui, W. H. and Tobak, M., "Bifurcation Analysis of Aircraft Pitching Motions at High Angles of Attack," *Jounal of Guidance and Control* , Vol. 7, 1984, pp. 106–113.
[40] Ioos G., Joseph D., *Elementary Stability and Bifurcation Theory*, Springer-Verlag, New York, 1980.
[41] Jahnke C. C., Culick F. E. C., Application of Bifurcation Theory to the High-Angle-of-Attack Dynamics of the F-14, *Journal of Aircraft*, 1994, Vol. 31, No. 1, pp.26-34.
[42] Jaramillo P., "An Analysis of Falling leaf Suppression Strategies for the F/A-18D," *AIAA Atmospheric Flight Mechanics Conference*, San Diego, July 29-30 1996.
[43] Jaramillo, P. and Ralston, J., "Simulation of the F/A-18D "Falling Leaf"," *AIAA Atmospheric Flight Mechanics Con- ference* , San Diego, July 28-30 1996.
[44] Jordan, T., Langford, W., Belcastro, C., Foster, J., Shah, G., Howland, G., and Kidd, R., "Development of a Dynamically Scaled Generic Transport Model Testbed for Flight Research Experiments," *AUVSI Unmanned Unlimited* , Arlington, VA, 2004.
[45] Kwatny H. G, et all.; Aircraft Accident Prevention: Loss-of-Control Analysis, AIAA Guidance, Navigation, and Control Conference 10 - 13 August 2009, Chicago, Illinois, AIAA 2009-6256 CP
[46] Kwatny, H. G. and Chang, B. C., "Constructing Linear Families from Parameter-Dependent Nonlinear Dynamics," *IEEE Transactions on Automatic Control* , Vol. 43, No. 8, 1998, pp. 1143–1147.
[47] Kwatny, H. G., Bennett, W. H., Berg, J. M., "Regulation of Relaxed Stability Aircraft," *IEEE Transactions on Automatic Control* , Vol. AC-36, No. 11, 1991, pp. 1325–1323.
[48] Kwatny, H. G., Chang, B. C., and Wang, S. P., "Static Bifurcation in Mechanical Control Systems," *Chaos and Bifurcation Control: Theory and Applications* , edited by G. Chen, Springer-Verlag, 2003.
[49] Lambregts, A. A., Nesemeier, G., Wilborn, J. E., and Newman, R. E., "Airplane Upsets: Old Problem, New Issues," *AIAA Modeling and Simulation Technologies Conference and Exhibit* , AIAA, Honolulu, Hawaii, 2008.
[50] Littleboy D. M., and Smith P. R., Using bifurcation methods to aid nonlinear dynamic inversion control law design. *J. Guidance, Navigation and Control*, Vol. 21, No. 4, pp. 632-638, 1998.
[51] Lowenberg M. H.. Bifurcation Analysis of Multiple-Attractor Flight Dynamics. *Phil. Trans. R. Soc.*, No. A 356, London, 1998, pp. 1745:2297-2319.
[52] Lowenberg, M. H. and Richardson, T. S., "The Continuation Design Framework for Nonlinear Aircraft Control," *AIAA Atmospheric Flight Mechanics Conference* , 2001.
[53] Lowenberg, M. H., "Bifurcation Analysis of Multiple-Attractor Flight Dynamics," *Philosphical Transactions: Mathemat- ical, Physical and Engineering Sciences* , Vol. 356, No. 1745, 1998, pp. 2297–2319.
[54] Lygeros, J., Tomlin, C., and Sastry, S., "Controllers for reachability specifications for hybrid systems," *Automatica* , Vol. 35, No. 3, 1999, pp. 349–370.
[55] Lygeros, J., "On Reachability and Minimum Cost Optimal Control," *Automatica* , Vol. 40, 2004, pp. 917–927.
[56] Marusak A. J., Pietrucha J. A., Sibilski K. S., Prediction of Aircraft Critical Flight Regimes Using Continuation and Bifurcation Methods, *38th Aerospace Sciences Meeting Technical Papers*, USA, 2000, AIAA-2000-0976-CP, American Institute of Aeronautics and Astronautics.
[57] Maryniak J, Maryniak A.: Pilot – człowiek w systemie sterowania samolotem i symulatorem lotu, *Mechanika w Lotnictwie*, PTMTiS Warszawa, 1994.
[58] Maryniak J., Goraj Z., Molicki W., Paturski Z.: Sterowność samolotu liniowego Ił-62M w stanach zagrożenia bezpieczeństwa, *Zbiór referatów XXVII Sympozjonu „Modelowanie w Mechanice"*, Gliwice, 1988.
[59] Maryniak J.: Dynamika samolotu z intensywnym oblodzeniem w locie na przykładzie TS-11

„ISKRA”, *Zeszyty Naukowe Katedry Mechaniki Stosowanej Politechniki Śląskiej*, XXXVIII Sympozjon „Modelowanie w Mechanice” zeszyt 7/99, Gliwice 1999.

[60] Masys. A; J.; Aviation accident aetiology: catastrophe theory perspective, Diasert Prevention and Management, Vo,. 13. No. 1, 2004, pp. 33-38

[61] Medina M., Shahaf M.: Post stall characteristics of highly augmented fighter aircraft, *Proceedings of 17-th ICAS Congress.* Stockholm, 1990.

[62] Mehra, R. K., Bifurcation analysis of aircraft high angle of attack flight dynamics, AIAA N 80-1599, August, 1980.

[63] Morelli, E. A. and DeLoach, R., “Wind Tunnel Database Development using Modern Experiment Design and Multivariate Orthogonal Functions,” *41s t AIAA Aerospace Sciences Meeting and Exhibit* , AIAA Paper 2003-0653, Reno, NV, January 2003.

[64] Morelli, E. A., “Global Nonlinear Aerodynamic Modeling Using Multivariate Orthogonal Functions,” *Journal of Aircraft* , Vol. 32, No. 2, 1995, pp. 270–277.

[65] Murch, A. M. and Foster, J. V., “Recent NASA Research on Aerodynamic Modeling of Post-Stall and Spin Dynamics of Large Transport Aircraft,” 8-11 January 2007.

[66] Namachivaya, N. S. and Ariaratnam, S., “Nonlinear Stability Analysis of Aircraft at High Angles of Attack,” *International Journal of Nonlinear Mechanics* , Vol. 21, No. 3, 1986, pp. 217–228.

[67] Nelson R. C., Jumper E. J.: Aircraft wake vortices and their effect on following aircraft, *AIAA 2001-4073CP*, Montreal, 2001.

[68] Nguyen L. T., et all.: Simulator study of stall/post-stall characteristics of a fighter aeroplane with relaxed longitudinal static stability, *NASA TP-1538* ,1979.

[69] Oishi M., Mitchell I. M., Tomlin, C., Saint-Pierre, P., “Computing Viable Sets and Reachable Sets to Design Feedback Linearizing Control Laws Under Saturation,” *45th IEEE Conference on Decision and Control*, IEEE, San Diego, 2006, pp. 3801–3807.

[70] Oprisiu C: Aircraft non-linear model in multivariable polynomial form for stability and control analysis (ICAS-94-7.8.4CP), *Proceedings 19th ICAS Congress*, 1994.

[71] Papadakis M., Alansatan S, See-Cheuk Wong.: Aerodynamic characteristics of a symmetric NACA section with simulated ice schapes, *AIAA 2000-0098CP*, Reno, 2000.

[72] Patten Van R., Supermaneuverability and Superagility, *Aeromedical and Training Digest*, Vol. 7 No. 1, Jan 1993.

[73] Planeaux, J. B. and Barth, T. J., High angle of attack dynamic behavior of a model high performance fighter aircraft, AIAA Paper 88-4368, August, 1988.

[74] Planeaux, J. B., Beck, J. A. and Baumann, D. D., Bifurcation analysis of a model fighter aircraft with control augmentation, AIAA Paper 90-2836, August, 1990.

[75] Pokhariyal D., Bragg M. B., Merret J.: Aircraft flight dynamics with simulated ice accretion, *AIAA-2001-0541CP*, Reno, 2001.

[76] Poston T, Steward I, Catastrophe theory and Its Application, Pitman, London, 1978

[77] Ranter, H., “Airliner Accident Statistics 2006,” Tech. rep., Aviation Safety Network, 2007.

[78] Raport NTSB , “Aircraft Accident Report; United Airlines Flight 232,” 1990.

[79] Raport NTSB: Aircraft Accident Report; Uncontrolled descent and collision with terrain USAir flight 427 Boeing 737-300, N513AU near Aliquippa, Pennsylvania, September 8, 1994,

[80] Reason J., Human Error, Cambridge University Press, Cambridge, 1990,

[81] Reason J., Managing the Risk of Organizational Accidents, Ashgate, Aldershot, 1998,

[82] Ritz L., Glasser H.: *Der Kältenwindkanal der Aerodynamischen Versuchsanstalt*, Göttingen, Luftwissen, Bd 5 N.1, 1938.

[83] Russell, P. and Pardee, J., “Final Report: JSAT Loss of Control: Results and Analysis,” Tech. rep., Federal Aviation Administration: Commercial Airline Safety Team, 2000.

[84] Sethian, J. A., “Evolution, Implementation, and Application of Level Set and Fast Marching Methods for Advancing Fronts,” *Journal of Computational Physics* , Vol. 169, 2001, pp. 503–555.

[85] Seydel R., *Practical Bifurcation and Stability Analysis: From Equilibrium to Chaos*, Springer-Verlag, 1994.

[86] Sibilski K., An Agile Aircraft Non-Linear Dynamics by Continuation Methods and Bifurcation Theory, *ICAS-2000-712, Proceedings of 22nd ICAS Congress*, Harrogate, UK, 2000.

[87] Sibilski K., Lasek M., Ładyżyńska-Kozdraś E., Maryniak J.: Aircraft climbing flight dynamics with simulated ice accretion”, *AIAA Meeting Papers on Disk*, vol. 9, no. 14-15, 2004, AIAA-2004- 4948CP.

[88] Sibilski K., Lasek M., Ładyżyńska-Kozdraś E., Maryniak J.: Aircraft climbing flight dynamics with simulated ice accretion”, *AIAA Meeting Papers on Disk*, vol. 9, no. 14-15, 2004, AIAA-2004- 4948CP.

[89] Sibilski K.: Numerical investigation into flight dynamics of an agile aircraft, *Journal of Theoretical and Applied Mechanics* Vol. 38, No. 1, 2000, str. 167-187.

[90] Sibilski K.: Numerical reconstruction of aircraft accidents flight dynamics, *Archives of Transport*, Vol. IX, No. 1-2, 1997.

[91] Sibilski K.: *Some thoughts on mathematical models for aircraft accidents simulation*, Aviation Safety H. Soekha (eds.), VSP Publishing Company, Utrecht, Holandia, 1997

[92] Sibilski K.: *Some thoughts on mathematical models*

for aircraft accidents simulation, Aviation Safety H. Soekha (eds.), VSP Publishing Company, Utrecht, Holandia, 1997

[93] Sinha N. K., and Ananthkrishnar N., Use of the Extended Bifurcation Analysis Method for Flight Control Law Design, *40th AIAA Aerospace Sciences Meeting*, USA, 2002, AIAA-2002-0249-CP, American Institute of Aeronautics and Astronautics.

[94] Smolicz T.: *Wpływ procesów decyzyjnych pilota na sterowanie samolotem komunikacyjnym podczas końcowej fazy zbliżania się do lądowania*, Rozprawa doktorska, Wydz. MEiL, PW, 1985.

[95] Soeder R. H., Sheldon D. W.: NASA Lewis icing research tunnel user manual, *NASA TM 107159*, 1996.

[96] Tobak M., Shiff L. B.: Aerodynamic mathematical modelling basic concepts, *AGARD-LS-114*, Lecture 1, 1981.

[97] Tomlin, C., Lygeros, J., and Sastry, S., "Aerodynamic Envelope Protection using Hybrid Control," *American Control Conference* , Philadelphia, 1998, pp. 1793–1796.

[98] Tran C. T., Petot D.: Semi-empirical model for the dynamic stall of airfoils in view of the application to the calculation of responses of a helicopter rotor blade in forward flight, *Vertica*, Nr. 5, 1981.

[99] Troger H., Steindl A., *Nonlinear Stability and Bifurcation Theory*, Springer Verlag, New York, 1991.

[100] Unnikrishnan S., Prasad, J. V. R., "Carefree Handling Using Reactionary Envelope Protection Method," *AIAA Guidance, Navigation and Control Conference and Exhibit* , Keystone, CO, 21-24 August 2006.

[101] Well, K. H., "Aircraft Control Laws for Envelope Protection," *AIAA Guidance, Navigation and Control Conference* , Keystone, Colorado, 21-24 August 2006

[102] Wiggins S., *Introduction to Applied Non-linear Dynamical Systems and Chaos*, Springer-Verlag, New York, 1990.

[103] Wilborn, J. E. and Foster, J. V., "Defining Commercial Aircraft Loss-of-Control: a Quantitative Approach," *AIAA Atmospheric Flight mechanics Conference and Exhibit* , AIAA, Providence, Rhode Island, 16-19 August 2004.

[104] Woodcock A., Davis M, Catastrrophe theory, Penguin Books, New York, 1978

[105] Woods D., Johannesen L., Cook R., Darter N., Behind Human Error Cognitive Systems, Computers, and Hindsight, Crew, System Ergonomics Information Analysis Center (CSERIAC), Wright Peterson Air Force Base, Dayton, OH, 1995

[106] Young J. W., Schy A. A., Johnson K. G.: Pseudosteady-state analysis of non-linear aircraft manoeuvres, *NASA TP 1758*, 1980.

[107] Young, J., Schy, A., and Johnson, K., "Prediction of Jump Phenomena in Aircraft Maneuvers Including Nonlinear Aerodynamics Effects," *Jounal of Guidance and Control* , Vol. 1, No. 1, 1978, pp. 26–31.

[108] Zagaynov, G. I. and Goman, M. G., Bifurcation analysis of critical aircraft flight regimes, ICAS-84-4.2.1, September, 1982

Copyright Statement